Confining Metal-Organic Framework Nanocrystals Within Mesoporous Materials: A General Approach via 'Solid-State' Synthesis.

Ignacio Luz, Mustapha Soukri*, and Marty Lail.

RTI International, Post Office Box 12194, Research Triangle Park, NC 27709-2194.

Overview.

1. Materials synthesis.

2. Material data sheets (MDS).

3. Characterization methods.

4. In situ experiments

5. Fourier Filtered Transformation (FFT) of STEM-HAADF images

1. Materials synthesis.

Chemicals

All chemicals were used as received from Sigma-Aldrich without further purification. $Cr(NO_3)_3 \cdot 9H_2O$, $CrCl_3 \cdot 6H_2O$, $Al(NO_3)_3 \cdot 9H_2O$, $AlCl_3 \cdot xH_2O$, $Co(NO_3)_2 \cdot 6H_2O$, $Ni(NO_3)_2 \cdot 6H_2O$, $ZrOCl_2 \cdot 8H_2O$, $RuCl_3 \cdot xH_2O$, $Zn(NO_3)_3 \cdot 9H_2O$, 1,4-benzenedicarboxylic acid (H_2BDC), 1,3,5-benzenetricarboxylic acid (H_3BTC), 2-aminoterephthalic acid ($H_2BDC(NH_2)$), monosodium 2-sulfoterephthalate ($H_2BDC(SO_3Na)$), 2,5-dihydroxyterephthalic acid (H_4DOBDC), 2,2′-Bipyridine-5,5′-dicarboxylic acid (H_2BpyDC), 2-methylimidazol (HMeIM), tetrakis(4-carboxyphenyl)-porphyrin (H_4TCPP). 1,3,6,8-tetrakis(p-benzoic acid)pyrene (H_4TBAPy) was synthetized according to the published procedure[1]. Triethylamine (TEA), *N*,*N*-dimethylformamide (DMF), tetrahydrofuran (THF) and methanol (MeOH) were of analytical grade (Sigma-Aldrich).

Mesoporous materials

Silica(A) [75-250 μm], Silica(B) [200-500 μm], Silica(C) [75-200 μm] and Silica(D) [75-150 μm] were kindly supplied by our commercial partner. SBA-15 was prepared according to the published procedure[2]. MCM-41 was provided by Claytec, γ-Al_2O_3 by Sasol, TiO_2 by Sachtleben and ZrO_2 by Mel Chemicals. Mesoporous carbon and HayeSep A (Supelco) [100-120 μm] were supplied by Sigma-Aldrich. All mesoporous materials were degassed at 120 °C overnight under vacuum to remove the adsorbed water. The particle size and morphology of the mesoporous materials are shown in Figure S1 and S2.

Ligand salt precursors

Na_2BDC and Na_3BTC ligand salt precursors were prepared from their acid form in water with the stoichiometric amount of NaOH necessary to deprotonate the carboxylic acid of the organic linker followed by a purification step via precipitation in acetone. Alternatively, ligand salt precursor solutions for $H_2BDC(NH_2)$, H_2BpyDC, H_4TCPP and H_4TBAPy were directly prepared with the stoichiometric amount of TEA, thereby skipping the step of isolating the ligand salt. $H_2BDC(SO_3Na)$ and HMeIM were directly dissolved in water. H_4DOBDC was dissolved in hot THF due to the insolubility in water of sodium 2,5-dioxyterephthalate coordination polymers and the formation in situ of triethylammonium salts did not give rise the targeted MOF-74 structure.

Bulk-type MOFs

For comparison purposes, the following MOFs were prepared and activated according to the reported literature: (Cr)MIL-101[3]/-53[4], (Cr)MIL-100[5], (Cr)MIL-101(SO_3H)[6], (Al)MIL-100[7], (Al)MIL-53(NH_2)[8], (Co, Ni)MOF-74[9,10],(Zr)UiO-66(H, NH_2)[11], (Zr)UiO-67(Bpy)[12], (Ru)HKUST-1[13], ZIF-8[14], PCN-222[15], NU-1000[1] and Co_2(dobpdc)[16]. FTIR spectra of these MOFs was used as reference for MOF/MPM hybrid materials. N_2 isotherms and pore distribution for (Cr)MIL-101(SO_3H) were included in Figure 1 in the manuscript. The rest of characterization data for bulk-type MOFs was not included in the Supplementary information.

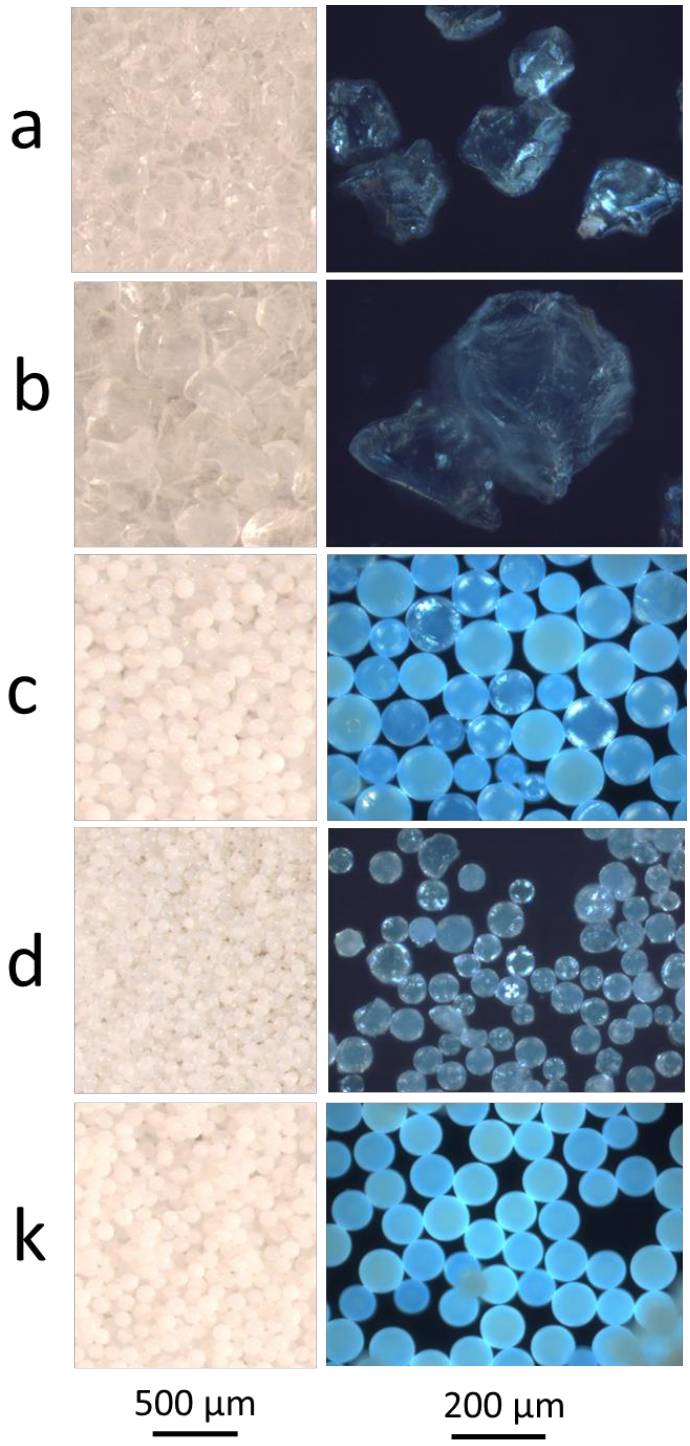

Figure S1. Optical (left columm) and confocal (right column) microscope images of Silica(A) (**a**, **MDS A2a)**, Silica(B) (**b**, **MDS A2b**), Silica(C) (**c**, **MDS A2c**), Silica(D) (**d**, **MDS A2d**) and HayeSep A (**k**, **MDS A2k**).

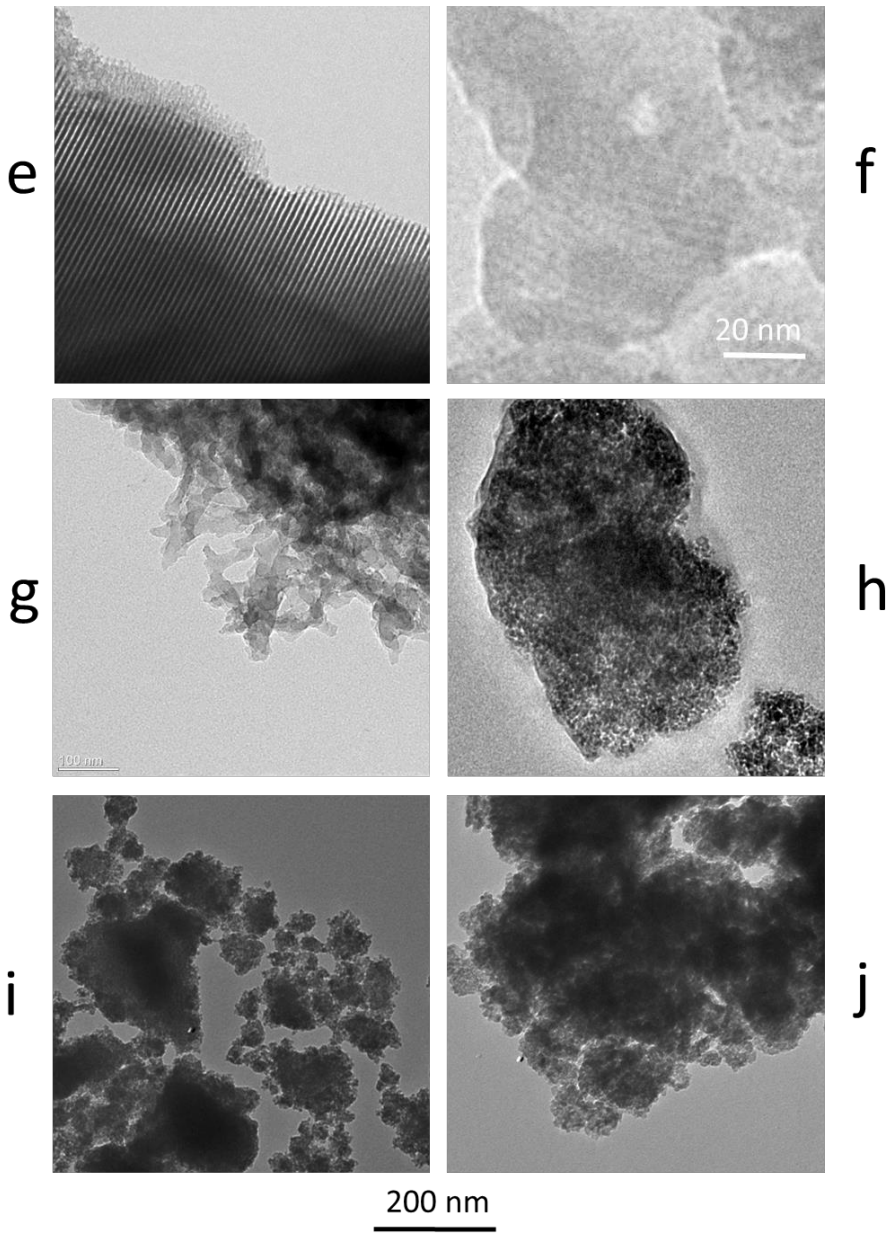

Figure S2. TEM images of SBA-15 (**e**, **MDS A2e)**, MCM-41 (**f**, **MDS A2f**), carbon (**g**, **MDS A2g**), γ-Al_2O_3 (**h**, **MDS A2h**), TiO_2 (**i**, **MDS A2i**) and ZrO_2 (**j**, **MDS A2j**). Scale bar for **f** is shown at the right bottom of the image.

General procedure for solid state synthesis of MOFs within MPMs

All MOF/MPM hybrid materials included in this work were prepared via solid-state synthesis by following the same general procedure: 1) sequential impregnation of MOF precursor solutions on MPMs, 2) treatment at specific conditions and 3) general washing treatment. MPMs were previously evacuated at 120 °C under vacuum for 24h. As illustrative example, the procedure and the resulting solid material obtained after the different steps for preparing 30 grams of (Cr)MIL-100/Silica(A) (MDS B1a) are illustrated in Figure S3.

Multistep incipient wetness impregnation (IWI) of MOF precursor solution on MPMs: first, the ligand salt precursor solution [$A_x(L^{-x})$] was impregnated to the evacuated MPM and was dried at 50 °C under vacuum in a rotavapor for 2 h (**S3a**). Subsequently, the resulting dry material [$A_x(L)^{-x}$/MPM] was placed in a tubular calcination reactor where was first treated with a nitrogen flow saturated with concentrated HCl (37%) for 2 hours at room temperature and after purged with a nitrogen flow for 2 h to remove the excess of HCl (**S3b, S3f**). Afterwards, the metal salt precursor solution $M_y(B^{-y})$ was impregnated to the compound [$H_x(L)^{-x}$/MPM]. The resulting solid [$M_y(B^{-y})/H_x(L^{-x})$/MPM] was finally dried at 50 °C under high vacuum in a rotavapor for 2 h (**S3c**). All the impregnation steps were done via incipient wetness impregnation. The amount and concentration of the solutions used per gram of MPMs are indicated in the Material Data Sheets for each specific hybrid material. M = metal; L = ligand; A = cation; B = anion.

Treatment at specific conditions: The dry solid [$M_y(B^{-y})/H_x(L^{-x})$/MPM] was placed either in a scintillation vial or Pyrex glass bottle capped with a Teflon tap for treatments at lower temperatures below 130 °C, or in a stainless-steel Parr autoclave for temperatures above 130 °C. A quantitative or catalytic amount of additive (such as water, DMF or TEA) was also added to the dry solid before the treatment (specified in MDSs). The specific conditions of temperature and time of synthesis for each hybrid MOF/MPM are also shown in MDSs in supporting information. In the case of trimethylamine (TEA) assisted synthesis, the dry material was placed in a tubular calcination reactor where was treated with a nitrogen flow saturated with TEA for 2 hours at room temperature and after purged with a nitrogen flow for 2 h to remove the excess of TEA, as done for acidification treatment with HCl (**S3f**).

*General washing procedure***:** After cooling the autoclave (**S3d**), the resulting products were thoroughly washed with distillated water or methanol in a filtration funnel. Subsequently, the material was washed overnight in a Soxhlet with MeOH (**S3e**). All the materials were activated overnight at 120 °C under vacuum.

An example: Multistep incipient wetness impregnation (IWI) for 19.1 wt% (Cr)MIL-101(SO_3H) precursor solution on mesoporous silica(A):

100 mL of an aqueous solution containing 20 g *$H_2BDC(SO_3Na)$* was impregnated to 50 grams of evacuated mesoporous silica(A) and was dried at 50 °C under vacuum in a rotavapor for 2 h. Subsequently, the resulting dry material [*$H_2BDC(SO_3Na)$*/SiO_2] was placed in a tubular calcination reactor where was first treated with a nitrogen flow saturated with concentrated HCl (37%) for 2 hours at room temperature and after purged with a nitrogen flow for 2 h to remove the excess of HCl. Afterwards, *75 mL of an aqueous solution containing 15 gr of* $Cr(NO_3)_3 \cdot 9H_2O$ in 75 mL of H_2O was impregnated to the compound [*$H_2BDC(SO_3H)$*/SiO_2]. The resulting solid [$Cr(NO_3)_3$/*$H_2BDC(SO_3H)$*/SiO_2] was finally dried at 50 °C under high vacuum in a rotavapor for 2 h. All the impregnation steps were done via incipient wetness impregnation. The solid [$Cr(NO_3)_3$/*$H_2BDC(SO_3H)$*/SiO_2] was separated in two 125 mL stainless steel Parr autoclave at 190 °C for 24 h after adjusting the water contain of the solid to 15-20 wt%. After cooling the autoclave, the resulting products were thoroughly washed with distillated water in a filtration funnel. Subsequently, the material was washed overnight in a Soxhlet with MeOH. All the materials were activated overnight at 120 °C under vacuum.

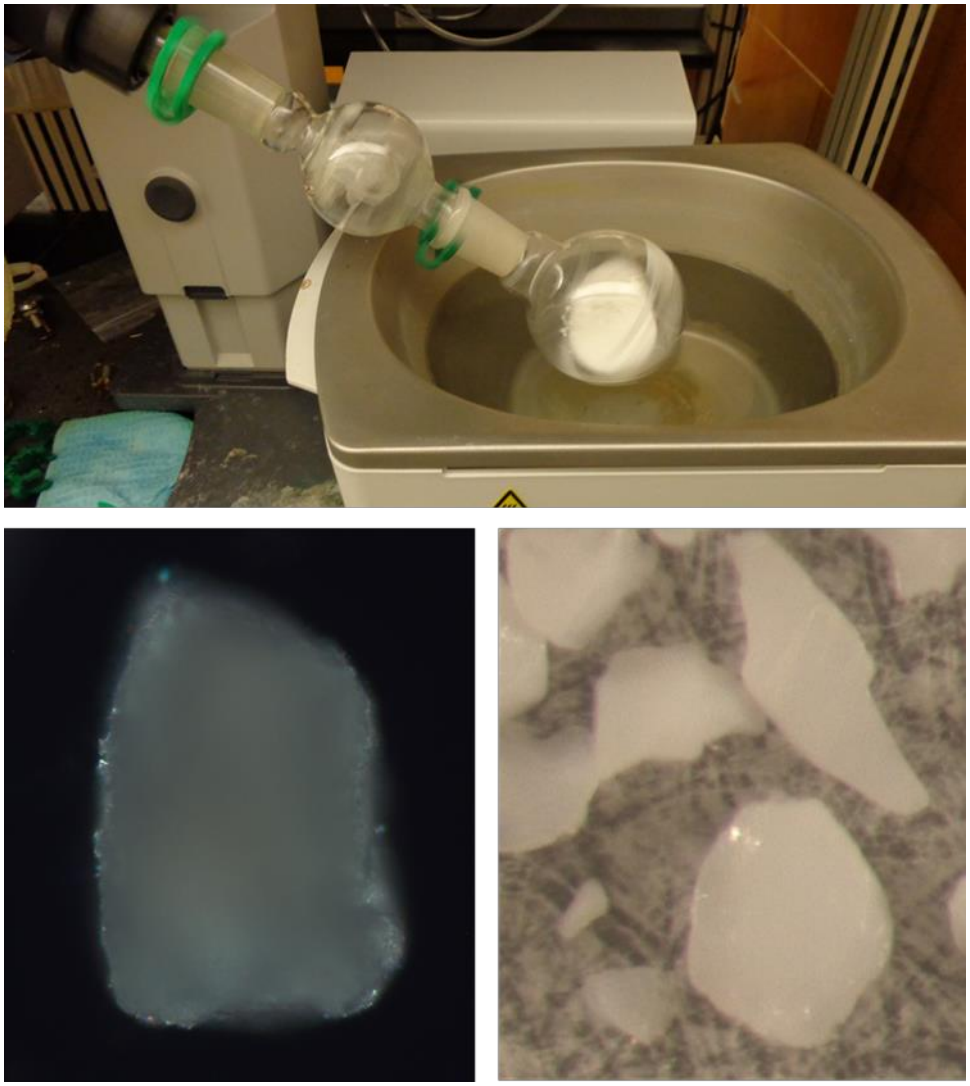

Figure S3a. Confocal and optical microscope images of the resulting material obtained from the impregnation of the ligand salt precursor (Na_3BTC) after drying in a rotavapor at 50 °C.

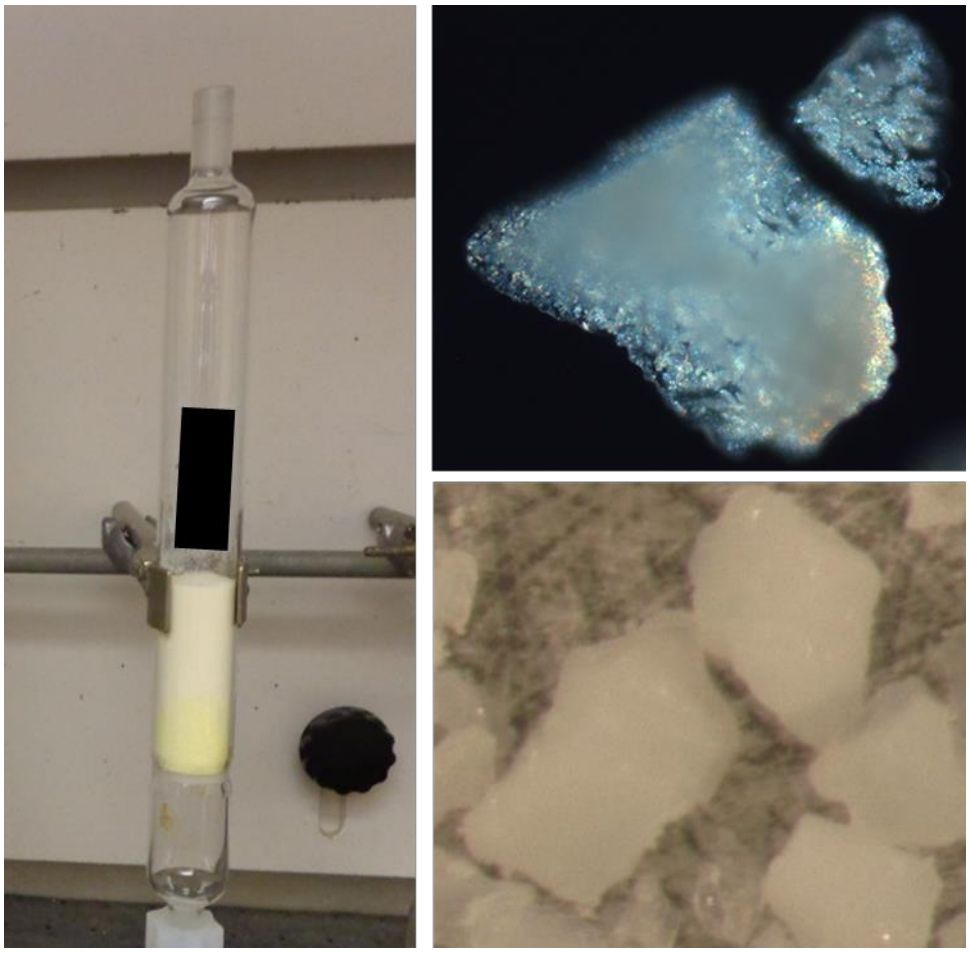

Figure S3b. Confocal and optical microscope images of the resulting material obtained from the acidification via gas phase of the ligand salt precursor (Na_3BTC) after evacuation under vacuum at 50 °C. Gas-phase acidification of the impregnated ligand $(TEA)_2BDC(NH_2)$ in a tubular calcination reactor is shown in the picture at the left due to the change of color from pale yellow (salt form) to bright yellow (acid form).

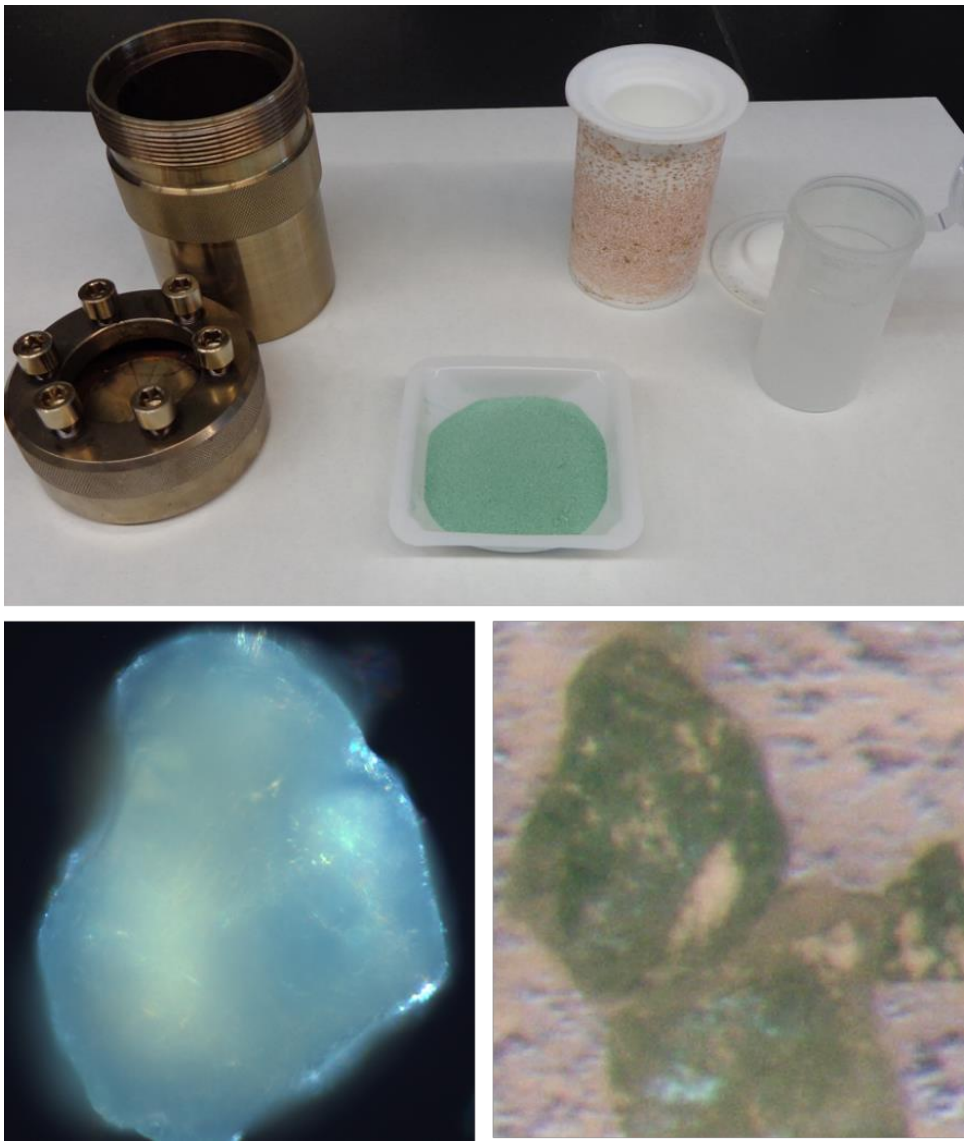

Figure S3c. Confocal and optical microscope images of the resulting material obtained from the impregnation of the metal salt precursor solution ($CrCl_3 \cdot 6H_2O$) after drying in a rotavapor at 50 °C. This dry powder containing 15 wt% H_2O was loaded in a 125 mL autoclave and heated at 200 °C for 2 h.

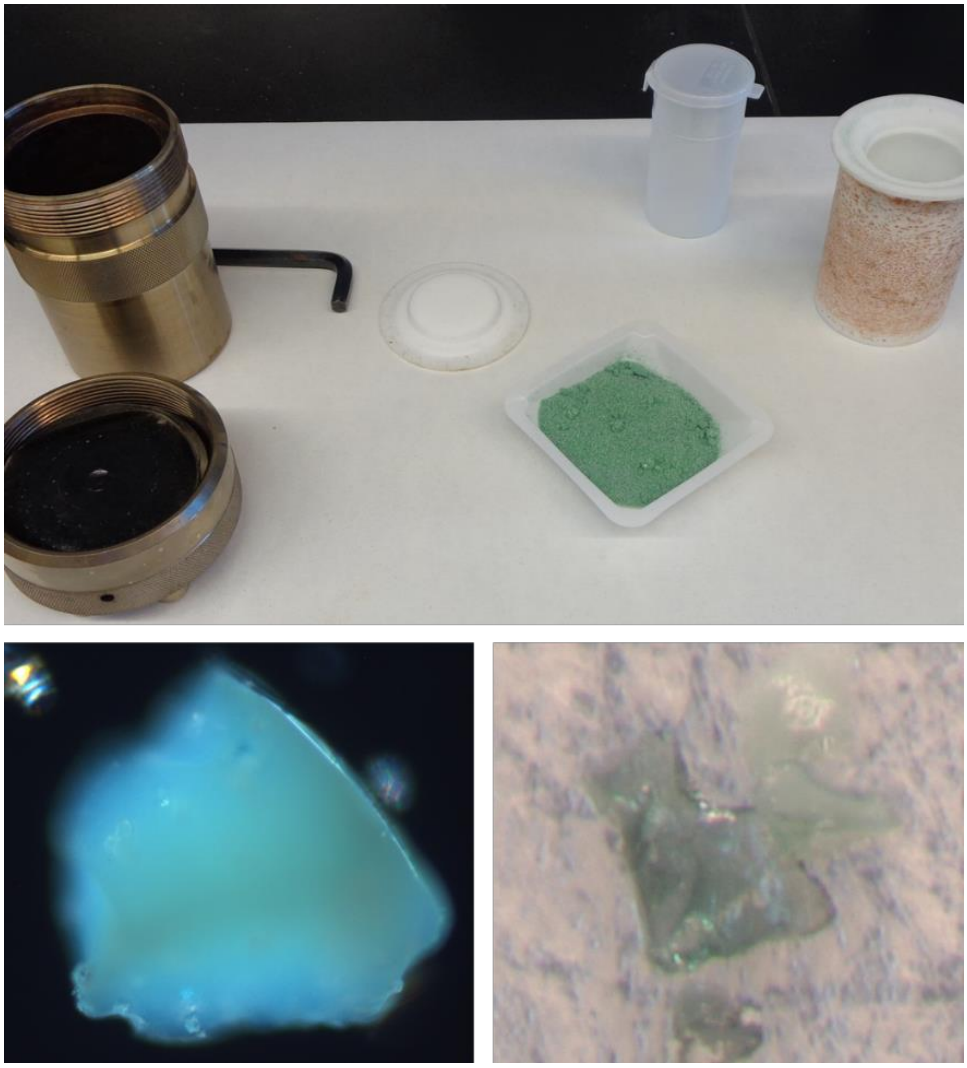

Figure S3d. Confocal and optical microscope images of the resulting material obtained after the heating treatment in the autoclave.

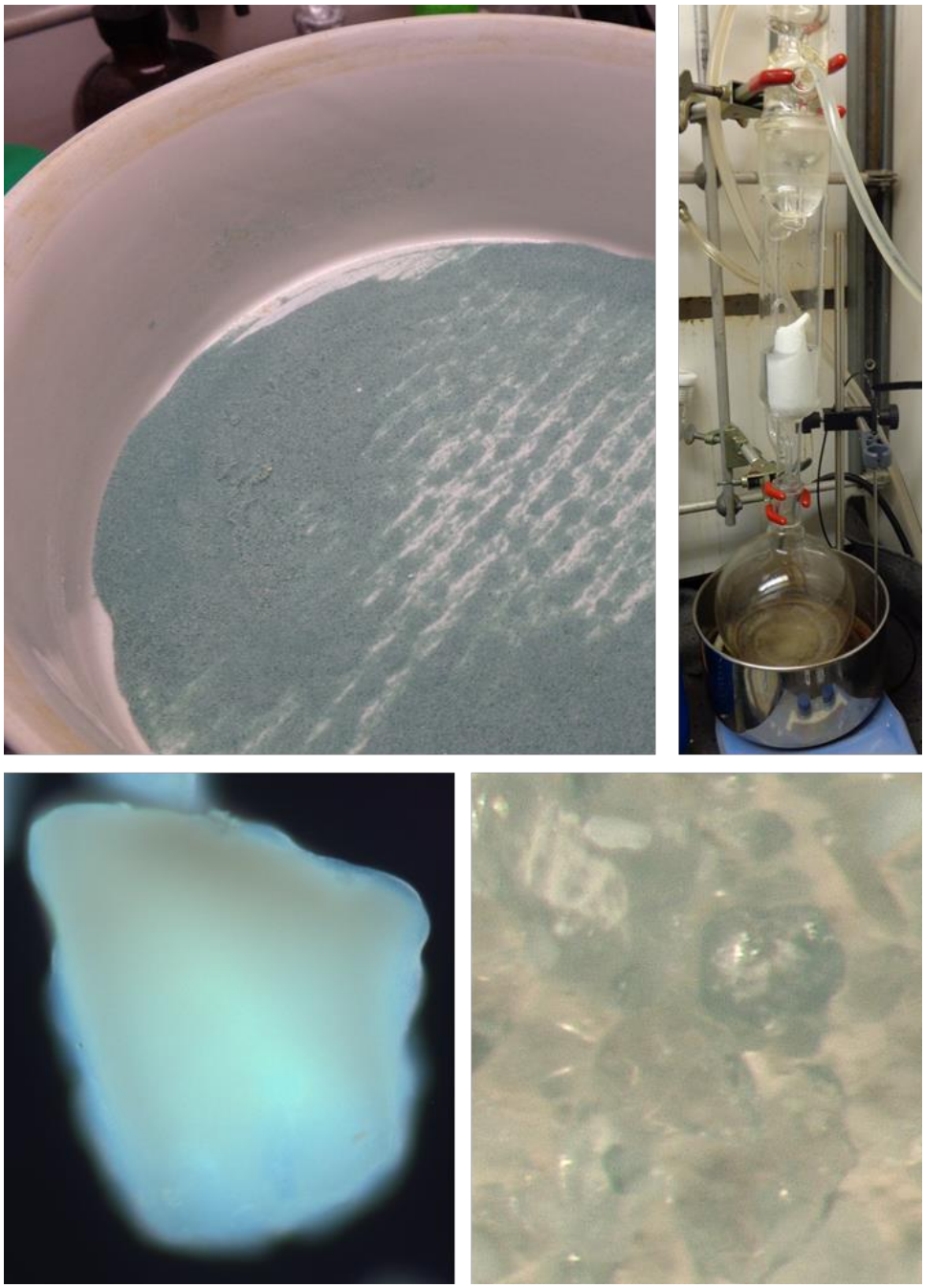

Figure S3e. Confocal and optical microscope images of the resulting material obtained from the general washing treatment.

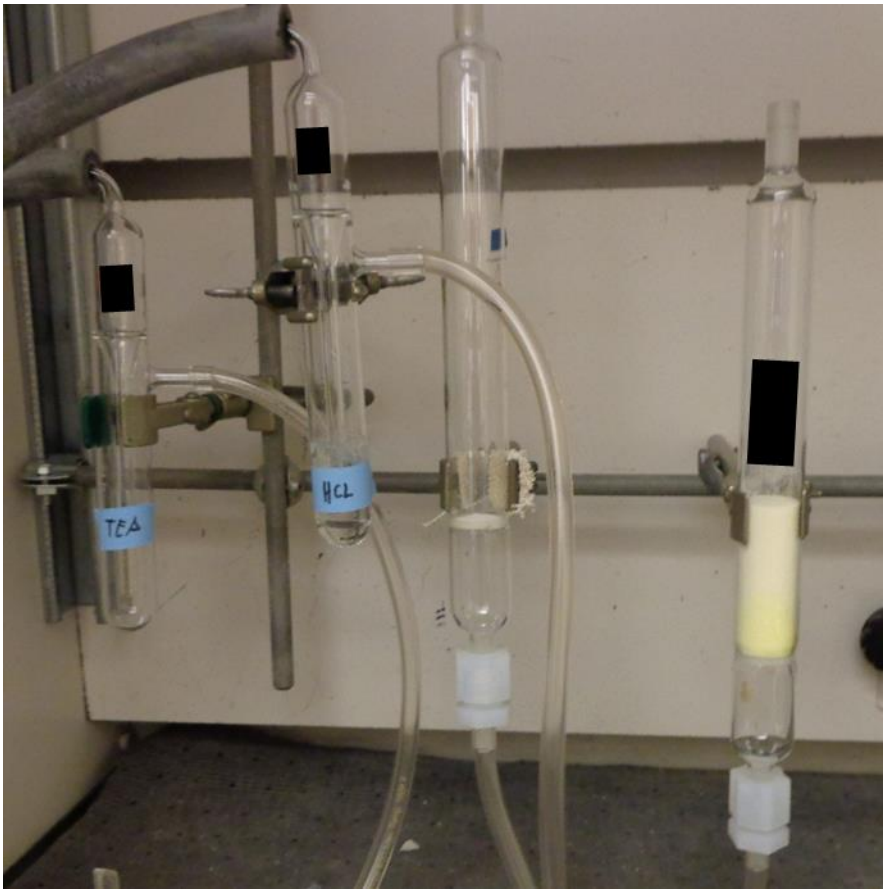

Figure S3f. Experimental set-up for gas-phase acidification and TEA treatment.

Figure 3g. MOF/Silica A material portfolio image**.**

Comparison with typical solvothermal synthesis.

An initial study consisting on a typical solvothermal (Cr)MIL-101 synthesis under the presence of Silica(A) at varying SiO_2/MOF ligand ratios (ranging from 15 to 45) reveals the poor adhesion of the MOF crystallites on the softly acid SiO_2 surface, thus leading to a highly heterogeneous sample, which shows the coexistence of empty SiO_2 particles and aggregates of MOF crystallites both free and on the SiO_2 outer surface. A SEM image (**S4a**) and confocal microscope image (**S4b**) of the resulting material after general washing procedure is shown in Figure S4. This non-selective MOF loading on SiO_2 using solvothermal conditions was likely found for other MOFs prepared using organic solvents as well, such as (Zr)PCN-222 (**S4c**). In the same way, non-selective MOF growth on the outer surface of MPMs is also obtained for some hybrid materials when the amount of additive is superior to 25 wt%, as shown for (Zr)UiO-66 (MDS E1a) when 50 wt% of H_2O was used (**S4d**). The specific synthesis conditions for the materials shown in Figure S4 are described below.

(Cr)MIL-101. 400 mg of $Cr(NO_3)_3 \cdot 9H_2O$, 166 mg of H_2BDC, 1 gr of Silica(A), 0.5 mL of acetic acid and 5mL of H_2O were mixed in a 50 mL autoclave and the synthesis was heated at 220 °C for 8 hours.

(Zr)PCN-222. 75 mg of $ZrOCl_2 \cdot 8H_2O$ and 100 mg of benzoic acid were dissolved in 10 mL of DMF and heated at 100 °C for 5 min. This solution was added to a scintillation vial containing 100 mg of Silica(A) and 25 mg of H_4TCPP in 10 mL of DMF. The mixture was heated at 120 °C for 24 hours. The confocal microscope image of the resulting material after general washing is shown in Figure S4c.

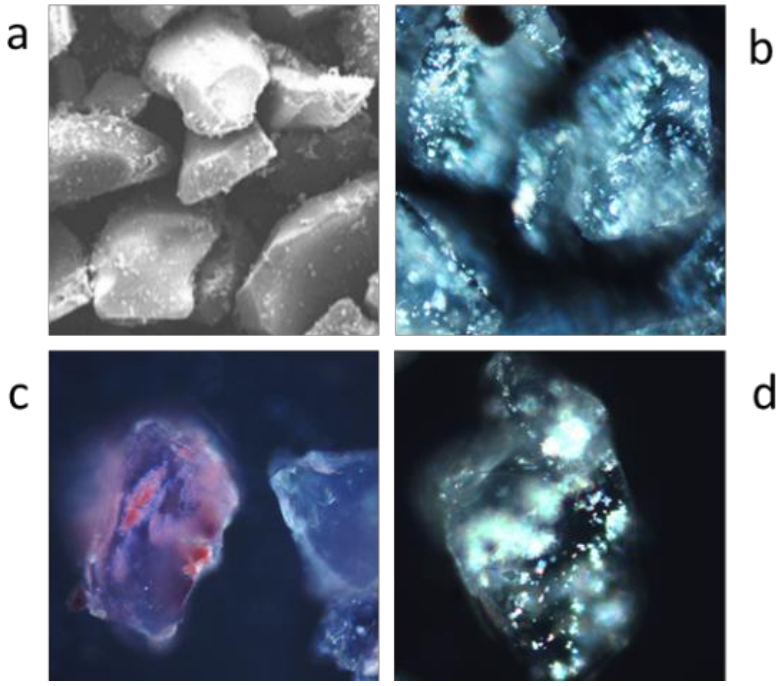

Figure S4. TEM (**4a**) and confocal microscope (**4b**) images for (Cr)MIL-100/Silica(A) prepared under solvothermal conditions. Confocal microscope image for (Zr)PCN-222/Silica(A) prepared under solvothermal conditions (**4c**). Confocal microscope image for (Zr)UiO-66/Silica(A) prepared using an excess of H_2O (50 wt%) via solid-state synthesis(**4d**).

Formation of non-porous coordination polymers: (Cr)MIL-101(SO_3H)/MPMs

MCM-41 (MDS A2f) exhibiting regular channels (2.5 nm) narrower than MOF cages (3.4 nm) was used for solid state synthesis of (Cr)MIL-101(SO_3H). According to the N_2 sorption isotherm, the mesopores are complete filled with an unknown phase exhibiting very low microporosity. At the same time, FTIR spectra shows a broadening down in energy for the $\nu_{as}(COO^-)$ antisymmetric stretching band from initial 1.620 to 1.580 cm^{-1} (see Figure 3c), which may be attributed to the coexistence of multiple isomeric forms exhibiting different distortion of the network. This shift down in the FTIR has been observed for (Cr)MIL-101(SO_3H)/Silica(A) prepared under the absence of additive This is accompanied with a drop in the microporosity measured by N_2 sorption isotherms (see Figure S5).

ZrO_2 (MDS A2j). ZrO_2 having tunable Lewis acidity-basicity and small pore size of 2.5 nm led to similar results as found for MCM-41 in terms of both the appearance of sharp micropore signals in the pore distribution plot and considerably lower surface area than the bare ZrO_2. FTIR spectra for ZrO_2 shows almost complete shift down of the carboxylic signal (due to almost absence of the vibration band at 1.620 corresponding to carboxylates bonded to Cr_3O clusters at (Cr)MIL-101(SO_3H) structure compared to γ-Al_2O_3, thus confirming the geometrical constrain that avoids the expansion of the framework to form the targeted MOF cavity.

TiO_2. In the case of TiO_2, which also exhibits an active surface but higher pore diameter (4 nm), surface area does not decrease as much as for ZrO_2 even containing similar loading of MOF precursors (13.0 and 14.4 wt%, respectively), the coexistence of a microporous material is not fully discarded. Furthermore, FTIR spectra for this hybrid material also reveals the presence of multiple species of carboxylate including the one corresponding to (Cr)MIL-101(SO_3H) phase at 1.620 cm^{-1}. Further studies will include other acid-basic mesoporous materials having pore diameters rather than 5 nm to confirm these hypotheses.

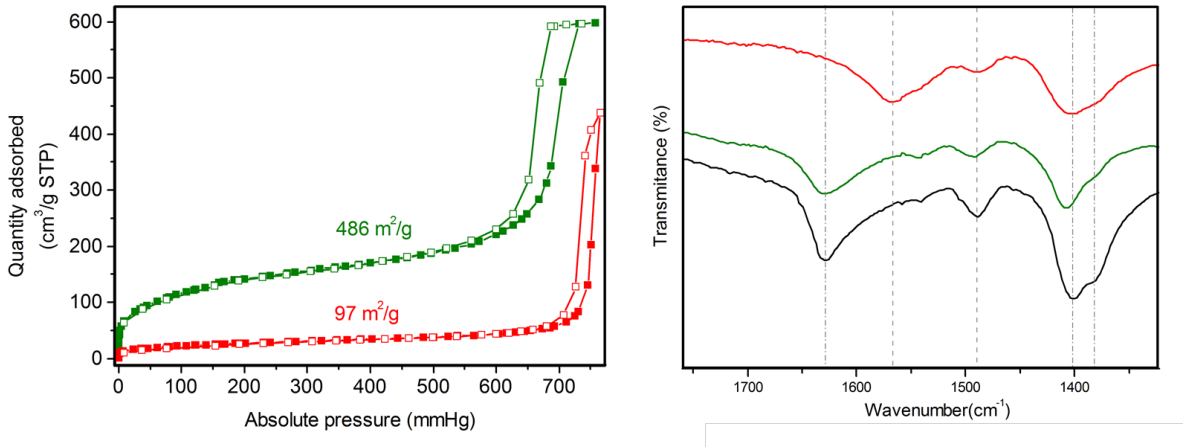

Figure S5. XRD and FTIR for (Cr)MIL-101(SO_3H)/Silica(A) obtained by using the optimized amount (15 wt%) of additive (green line) and any additive (red line), which led to non-porous coordination polymer. The black line corresponds to the reference MOF.

2. Materials data sheets (MDS)

The MDSs show the characterization routine carried out for all the MOF/MPM hybrid materials shown in this work. Each material data sheet gathers the following information:

<table>
<tr>
<td>MDS code [XYz]
(X = MOF structure; Y = metal/ligand; z = MPM)
MOF/MPM
MOF molecular formula
[molecular weight; metal contain (wt%)]
Ligand salt precursor solution:
volume of solution added in the 1st IWI per gram of MPM
Metal salt precursor solution:
volume of solution added in the 3rd IWI per gram of MPM
Trace of solvent: amount of additive per gram of the resulting solid after IWI (MOF precursors loaded on MPM)
Synthesis conditions: temperature and time of synthesis
XRF: loading of MOF according to X-ray fluorescence (stoichiometric loading of MOF according to the theoretical formula)
MOF yield
TGA: wt% loading of MOF according to organic loss
Surface area: calculated by BET method from N_2 isotherms</td>
<td>Optical microscope image</td>
</tr>
<tr>
<td>Z-confocal or TEM microscope image</td>
<td>XRD pattern
MOF/MPM (colored line)
Simulated MOF (black line)</td>
</tr>
<tr>
<td>FTIR spectra
MOF precursor loaded on MPM (red line)
bare MPM (grey line)
MOF/MPM (colored line)
MOF reference (black line)</td>
<td>N_2 sorption isotherm and pore distribution[b]
MOF/MPM (colored line)
MPM (grey line)</td>
</tr>
</table>

[a] Specifications. [b] Calculated by BJH adsorption dV/dD plot (inset figure; pore diameter (nm) at X-axis and pore volume ($cm^3 g^{-1} nm^{-1}$) at Y axis).

Index MDS

- *MDS-1*
  - *A1a → (Cr)MIL-101/Silica(A)*
  - *B1a → (Cr)MIL-100/Silica(A)*
  - *B2a → (Al)MIL-100/Silica(A)*
  - *C1a → (Cr)MIL-53/Silica(A)*
  - *C2a → (Al)MIL-53(NH_2)/Silica(A)*
  - *D1a → (Co)MOF-74/Silica(A)*
  - *D2a → (Ni)MOF-74/Silica(A)*
  - *E1a → (Zr)UiO-66/Silica(A)*
  - *E2a → (Zr)UiO-66(NH_2)/Silica(A)*
  - *F1a → (Zr)UiO-67(Bpy)/Silica(A)*
  - *G1a → (Zn)ZIF-8/Silica(A)*
  - *H1a → (Cu)HKUST-1/Silica(A)*
  - *H2a → (Ru)HKUST-1/Silica(A)*
  - *I1a → (Zr)PCN-222/Silica(A)*
  - *J1a → (Zr)NU-1000/Silica(A)*
  - *K1a → Co_2(DOBPDC)/Silica(A)*

- *MDS-2*
  - *A2a → (Cr)MIL-101(SO_3H)/Silica(A)*
  - *A2b → (Cr)MIL-101(SO_3H)/Silica(B)*
  - *A2c → (Cr)MIL-101(SO_3H)/Silica(C)*
  - *A2d → (Cr)MIL-101(SO_3H)/Silica(D)*
  - *A2e → (Cr)MIL-101(SO_3H)/SBA-15*
  - *A2f → (Cr)MIL-101(SO_3H)/MCM-41*
  - *A2g → (Cr)MIL-101(SO_3H)/Carbon*
  - *A2h → (Cr)MIL-101(SO_3H)/γ-Al_2O_3*
  - *A2i → (Cr)MIL-101(SO_3H)/TiO_2*
  - *A2j → (Cr)MIL-101(SO_3H)/ZrO_2*
  - *A2k → (Cr)MIL-101(SO_3H)/HayeSep A*

MDS A1a

(Cr)MIL-101(H)/Silica(A)

$Cr_3O(OH)(BDC)_3 \cdot 2(H_2O)$

[MW=717, 21.7 wt% Cr]

Ligand salt precursor solution*:*

2 mL of 200 mg *Na_2BDC* / mL H_2O

Metal salt precursor solution:

1.5 mL of 480 mg *$Cr(NO_3)_3 \cdot 9H_2O$* / mL H_2O

Trace of solvent: 15 wt% H_2O

Synthesis conditions: 220 °C for 1 h

XRF: 30.8% MOF (43.0 wt% max)

Yield = 71.6 %

TGA: 14.2 wt% weightloss (organic)

Surface area: 584 m^2/g

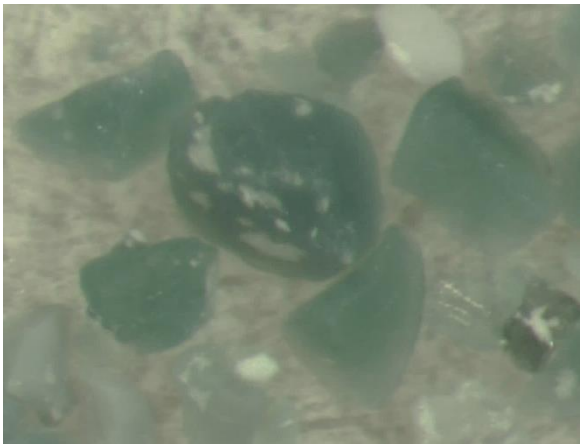

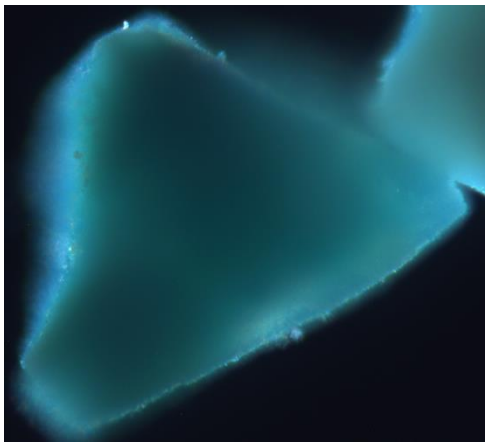

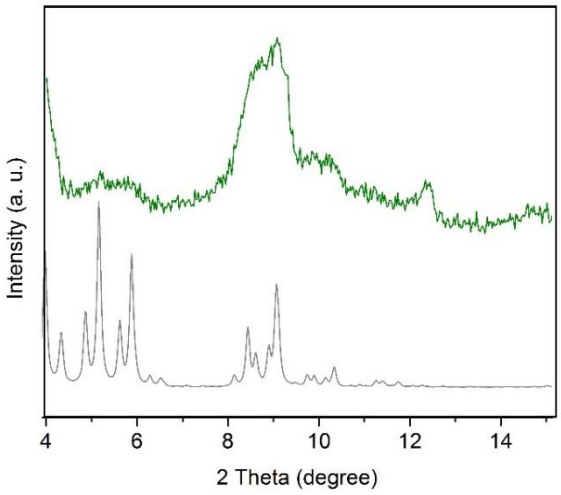

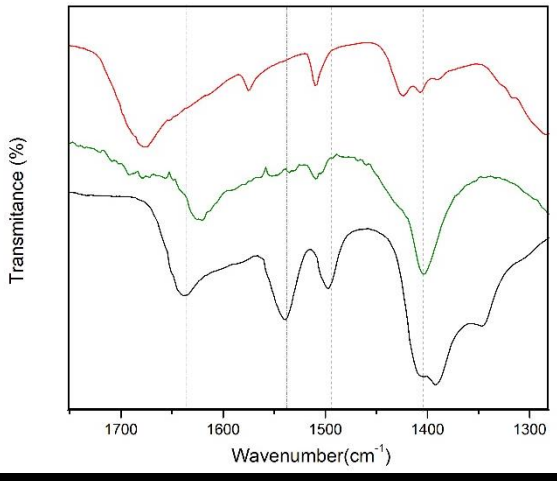

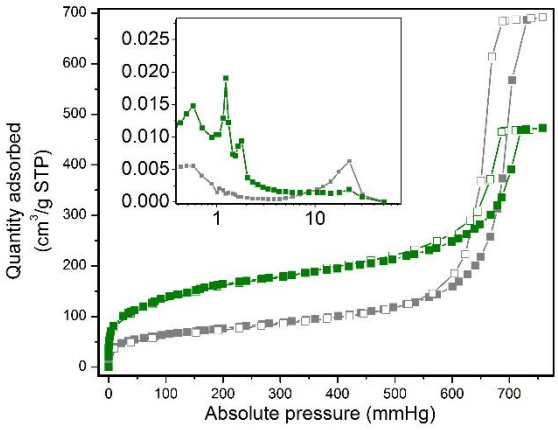

MDS B1a

(Cr)MIL-100/ Silica(A)

$Cr_3OCl(BTC)_2 \cdot 2(H_2O)$ [MW=664, 23.4 wt% Cr]

Ligand salt precursor solution*:*

2 mL of 200 mg *$Na_3(BTC)$* / mL H_2O

Metal salt precursor solution*:*

1.5 mL of 400 mg *$CrCl_3 \cdot 6H_2O$* / mL H_2O

Trace of solvent: 15 wt% H_2O

Synthesis conditions: 200 °C for 2 h

XRF: 35.0 wt% MOF (47.5 wt% max)

Yield = 73.6%

TGA: 14.4 % weightloss (organic)

Surface area: 647 m^2/g

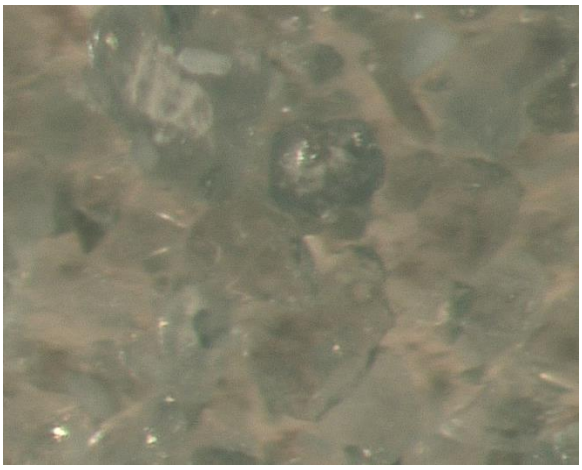

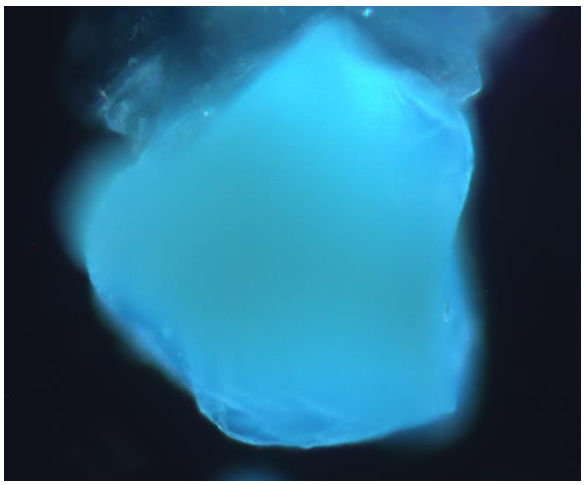

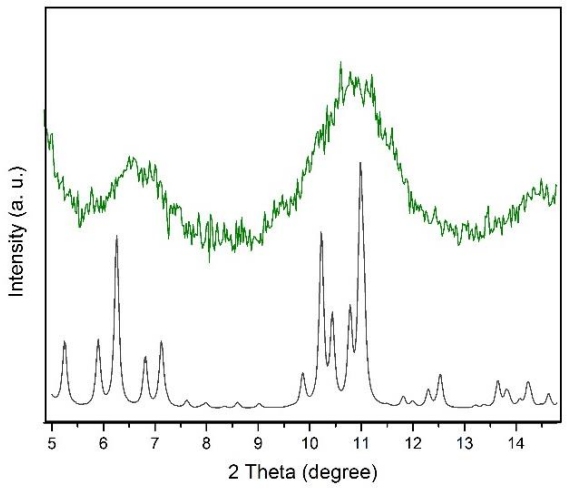

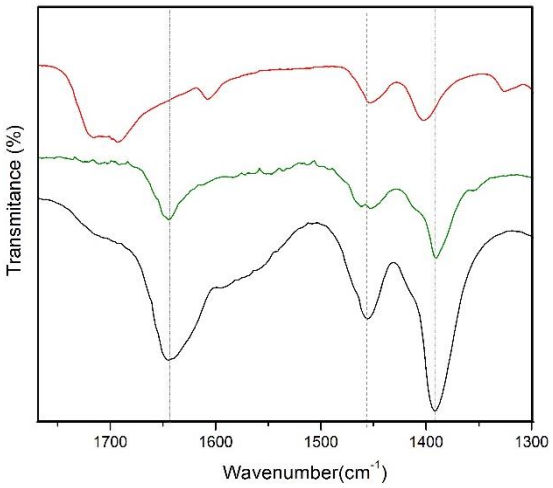

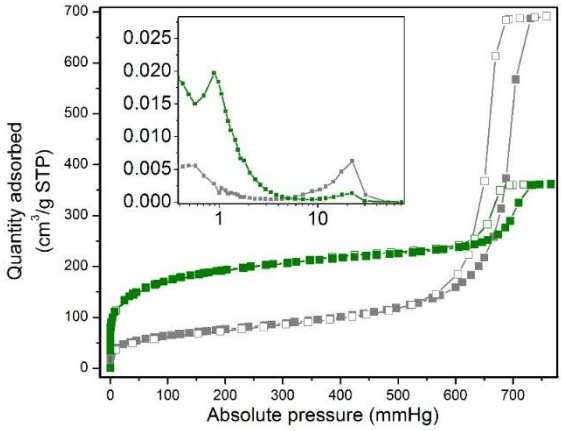

MDS B2a
(Al)MIL-100/ Silica(A)
$Al_3OCl\ (BTC)_2 \cdot 2H_2O$ [MW=590, 13.7 wt% Al]
Ligand salt precursor solution*:*
2 mL of 200 mg *$Na_3(BTC)$* / mL H_2O
Metal salt precursor solution*:*
1.5 mL of 530 mg *$Al(NO_3)_3 \cdot 9H_2O$* / mL H_2O
Trace of solvent: 15 wt% H_2O
Synthesis conditions: 200 °C for 8 h
XRF: 20.4 wt% MOF (42.3 wt% max)
Yield = 48.2 %
TGA: 14.2 wt% weight loss (organic)
Surface area: 364 m^2/g

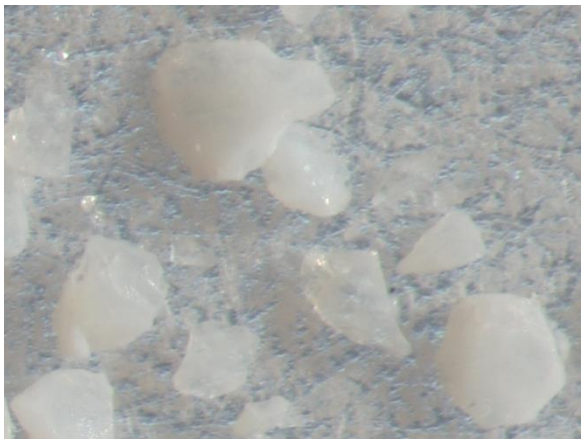

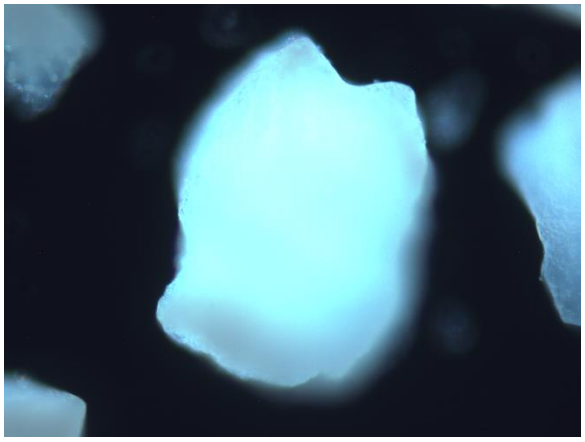

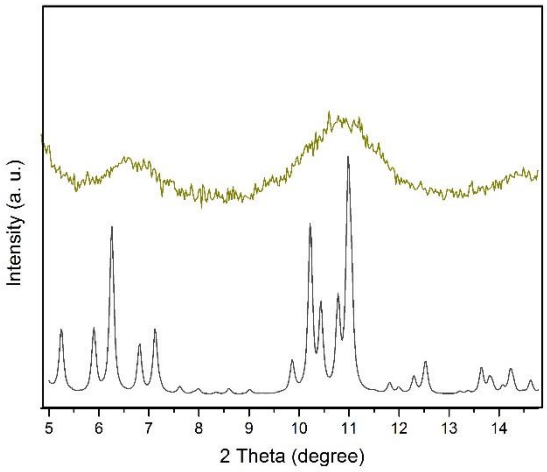

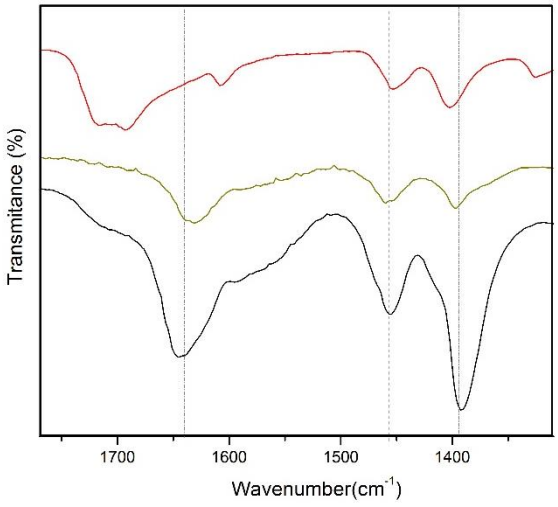

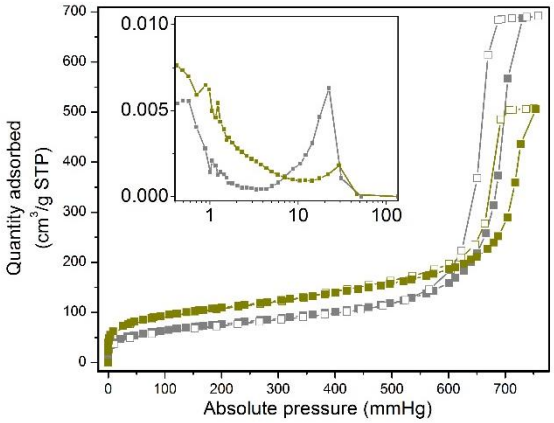

MDS C1a

(Cr)MIL-53/ Silica(A)

Cr(OH) (BDC) [MW=233, 22.3 wt% Cr]

Ligand salt precursor solution*:*

2 mL of 150 mg *$Na_2(BDC)$* / mL H_2O

Metal salt precursor solution*:*

1.5 mL of 360 mg *$Cr(NO_3)_3{\cdot}9H_2O$* / mL H_2O

Trace of solvent: 15 wt% H_2O

Synthesis conditions: 220 °C for 12 h

XRF: 22.7 wt% MOF (31.4 wt% max)

Yield = 72.2 %

TGA: 13.6 wt% weight loss (organic)

Surface area: 377 m^2/g

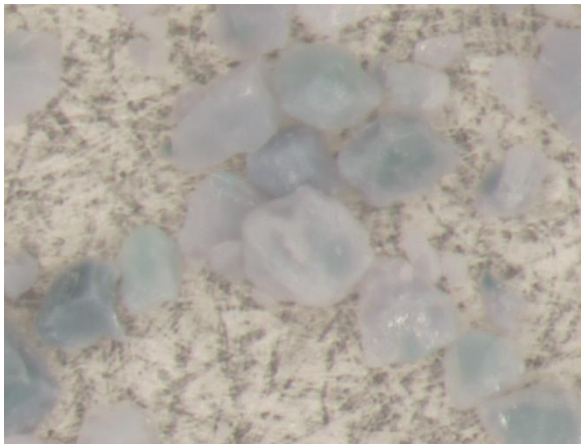

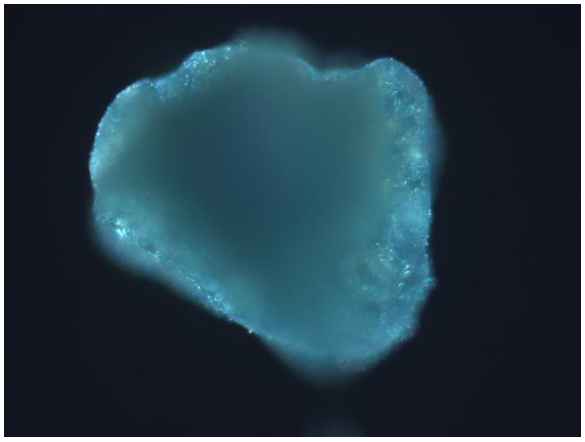

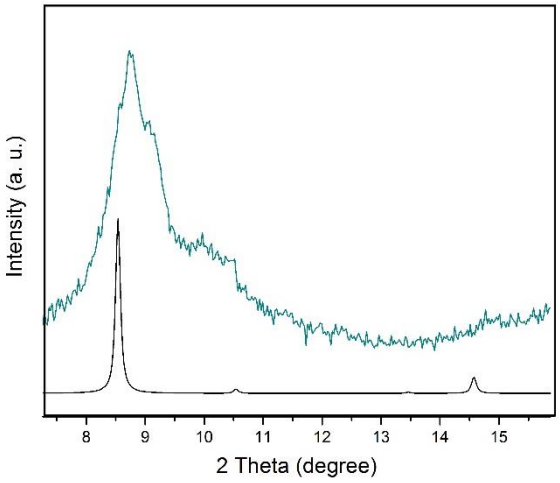

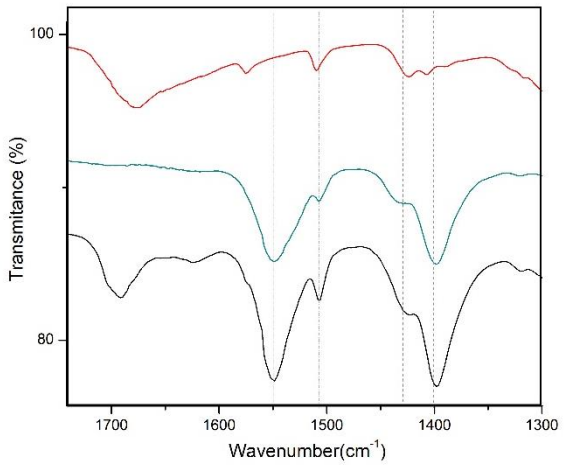

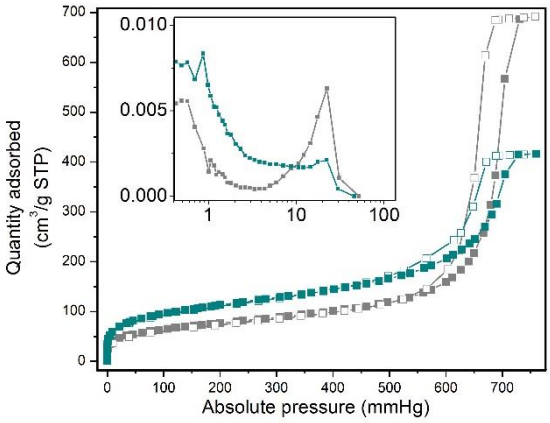

MDS C2a

(Al)MIL-53(NH_2)/ Silica(A)

Al(OH) (BDC(NH_2)) [MW=223, 12.1 wt% Cr]

Ligand salt precursor solution*:*

2 mL of 150 mg $H_2BDC(NH_2)$ + 175 µL TEA / 1 mL H_2O

Metal salt precursor solution*:*

1.5 mL of 400 mg/mL $Al(NO_3)_3 \cdot 9H_2O$ / 1 mL H_2O

Trace of solvent: 15 wt% DMF

Synthesis conditions: 120 °C for 12 h

XRF: 28.7 wt% MOF (37.2 wt% max)

Yield = 77.1%

TGA: 14.4 wt% weight loss (organic)

Surface area: 417 m^2/g

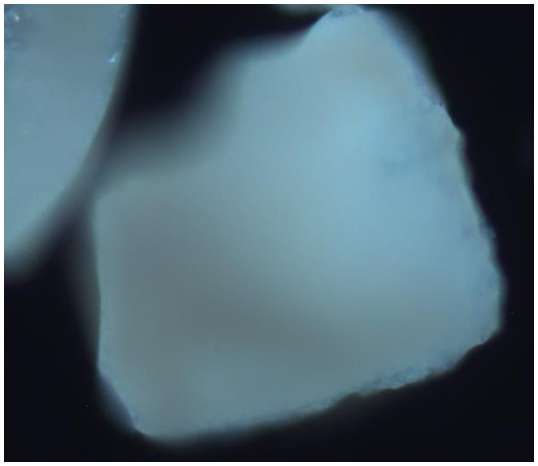

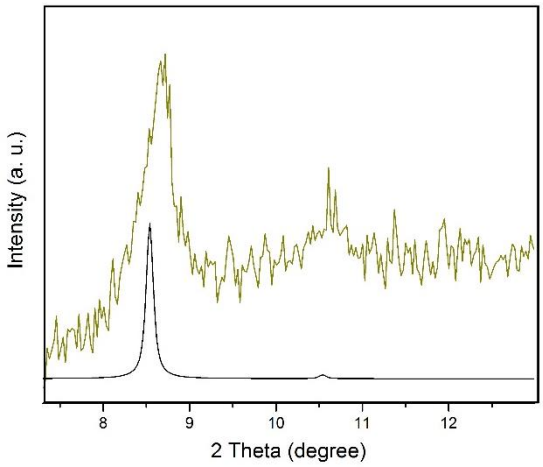

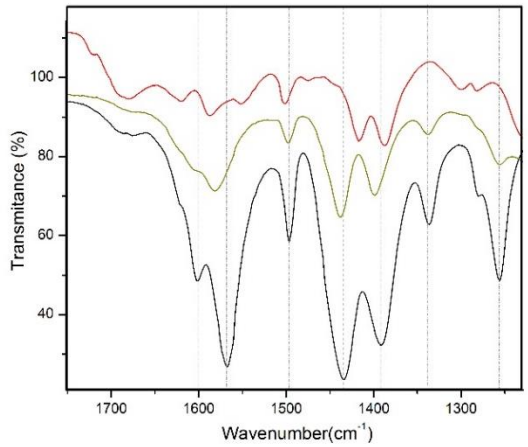

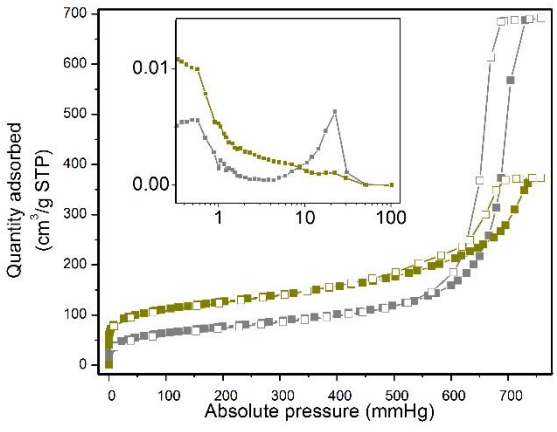

MDS D1a

(Co)MOF-74/ Silica(A)

$Co_2(DOBDC)\cdot 2(H_2O)$ [MW=348; 33.9 wt% Co]

Ligand salt precursor solution*:*

4 mL of 50 mg *H_4DOBDC*/ mL THF[a]

Metal salt precursor solution*:*

1.5 mL of 400 mg *$Co(NO_3)_2\cdot 6H_2O$* / mL H_2O

Trace of solvent: vapor of Et_3N

Synthesis conditions: RT for 1 hour

XRF: 27.3 wt% MOF (35.1 wt% max)

Yield = 77.7%

TGA = 12.1 wt% organic

Surface area: 324 m^2/g

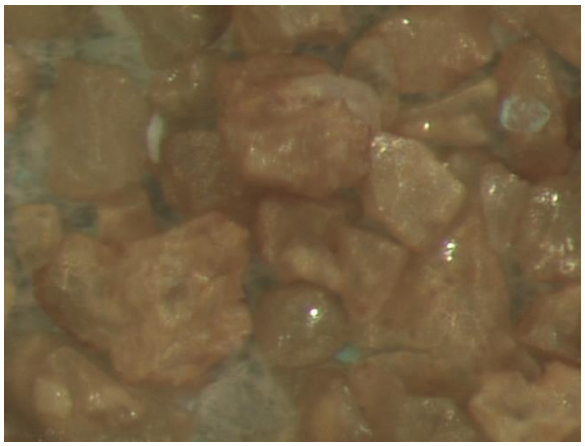

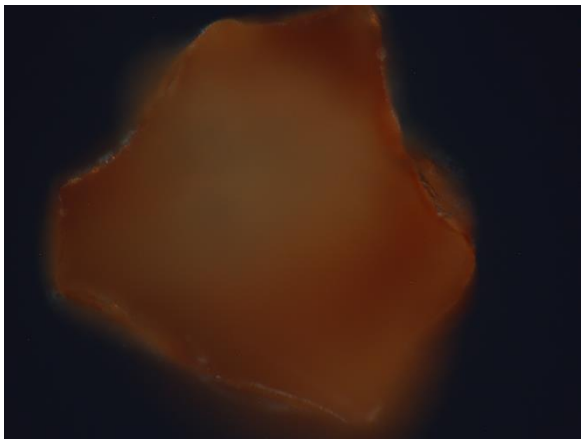

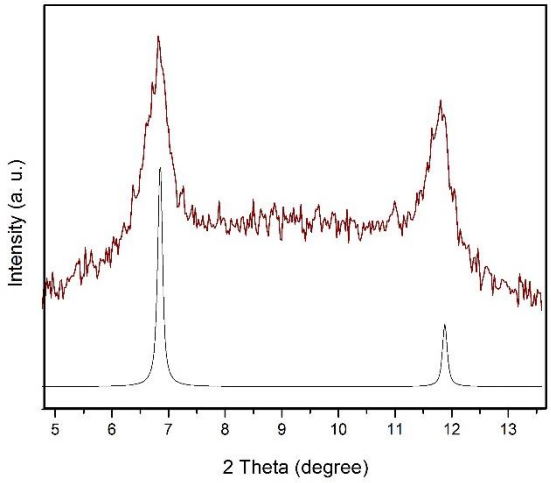

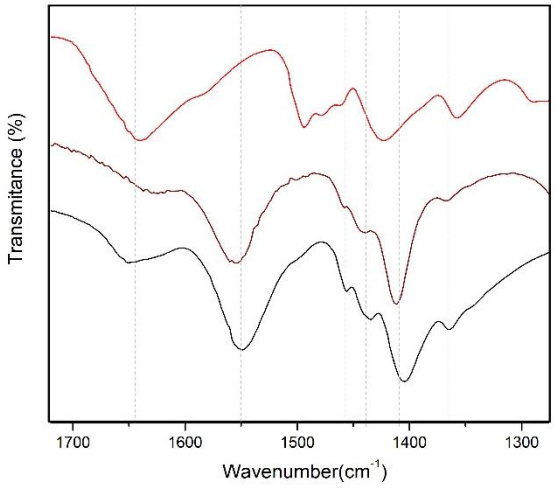

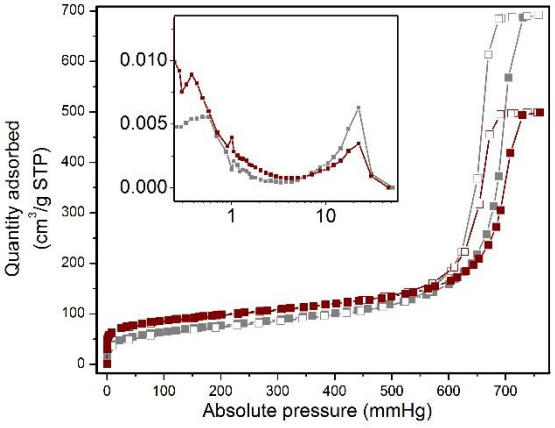

[a] *Double IWI for ligand impregnation / evacuation is required for MOF-74 materials, since ligand sodium ligand salt led to non-soluble coordination polymer and triethylammonium ligand salt led to other crystalline phase upon exposure to the metal precursor.*

MDS D2a

(Ni)MOF-74/ Silica(A)

$Ni_2(DOBDC)\ 2(H_2O)$ [MW=347; 33.1 wt% Ni]

Ligand salt precursor solution*:*

4 mL of 50 mg *H_4DOBDC* / mL THF[a]

Metal salt precursor solution

1.5 mL of 400 mg *$Ni(NO_3)_2{\cdot}6H_2O$* / mL H_2O

Trace of solvent: vapor of Et_3N

Synthesis conditions: RT for 1 hour

XRF: 27.7 wt% MOF (35.0 wt% max)

Yield = 79.1%

TGA = 11.6 wt% weightloss (organic)

Surface area: 386 m^2/g

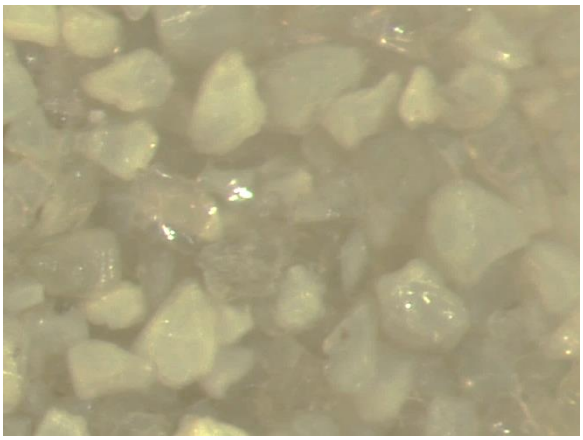

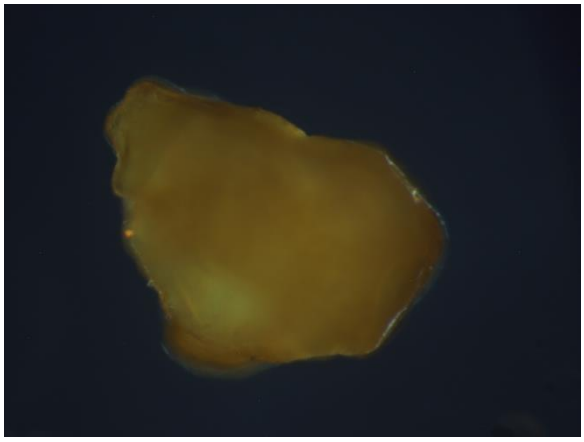

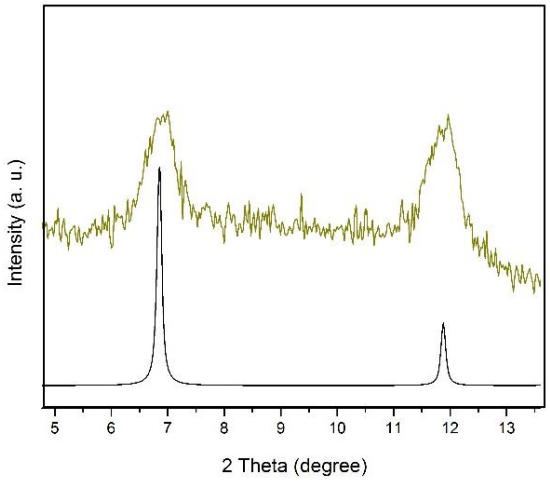

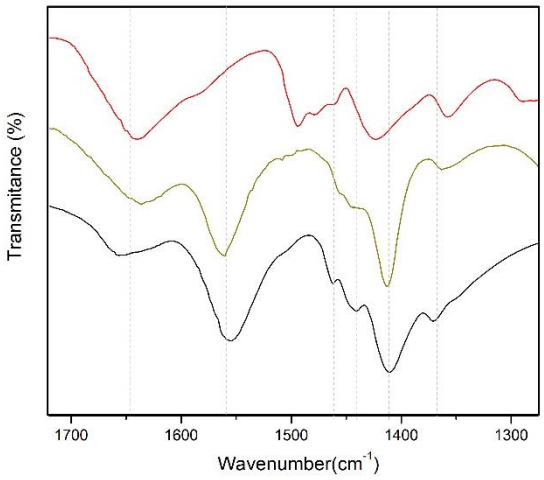

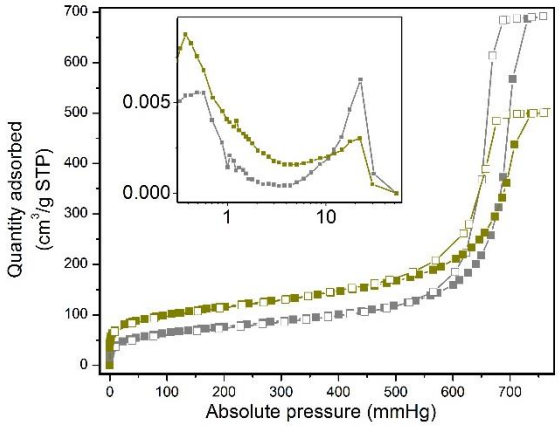

[a] *Double IWI for ligand impregnation / evacuation is required for MOF-74 materials, since ligand sodium ligand salt led to non-soluble coordination polymer and triethylammonium ligand salt led to other crystalline phase upon exposure to the metal precursor*

MDS E1a

(Zr)UiO-66/ Silica(A)

$Zr_6O_4(OH)_4(BDC)_6$ [MW=1662, 32.8 wt% Zr]

Ligand salt precursor solution*:*

2 mL of 150 mg $Na_2(BDC)$ / mL H_2O

Metal salt precursor solution*:*

1.5 mL of 330 mg $ZrOCl_2{\cdot}8H_2O$ / mL H_2O

Trace of solvent: 15 wt%H_2O

Synthesis conditions: 120 °C for 2 hours

XRF: 30.0 wt% MOF (39.5 wt% max)

Yield = 75.9%

TGA: 12.3% weightloss (organic)

Surface area: 363 m^2/g

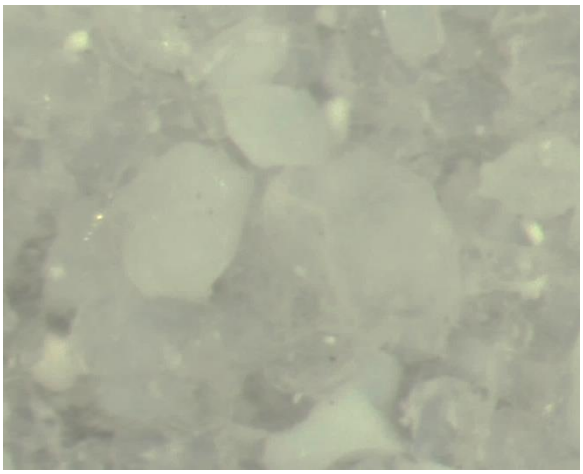

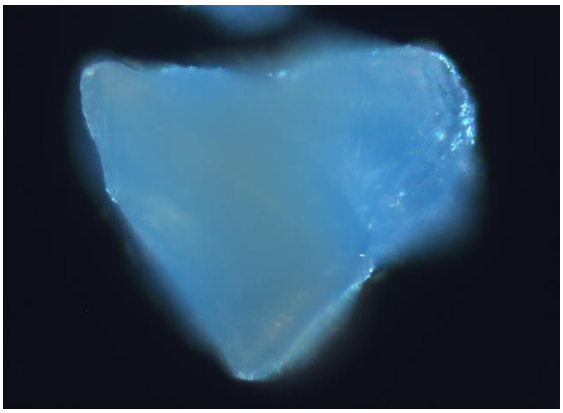

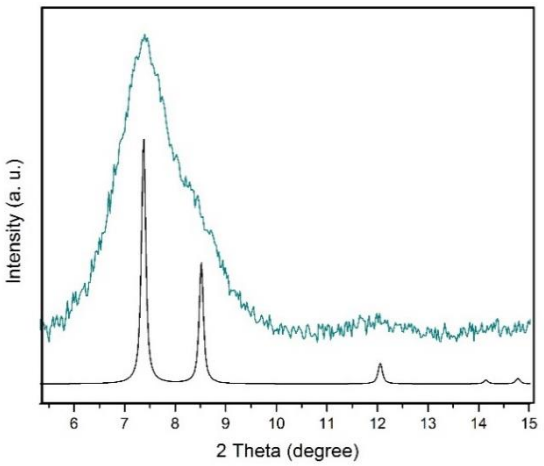

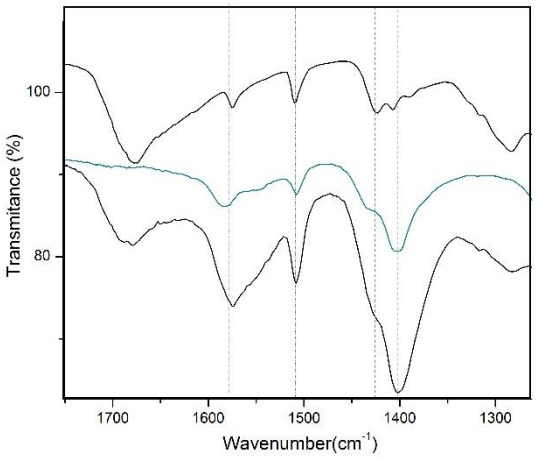

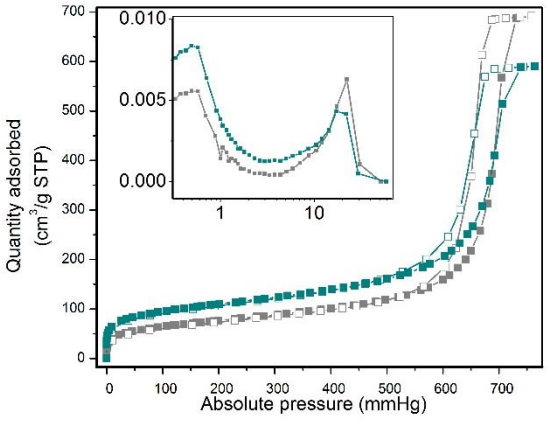

MDS E2a

(Zr)UiO-66(NH_2)/ Silica(A)

$Zr_6O_4(OH)_4$(BDC-NH_2)$_6$ [MW=1764, 30.9 wt% Zr]

Ligand salt precursor solution*:*

2 mL of 150 mg $H_2BDC(NH_2)$+235 µL TEA/ mL H_2O

Metal salt precursor solution:

1.5 mL of 330 mg $ZrOCl_2{\cdot}8H_2O$ / mL H_2O

Trace of solvent: 15 wt%H_2O

Synthesis conditions: 120 °C for 2 hours

XRF: 37.6 wt% MOF (43.1 wt% max)

Yield = 87.1 %

TGA: 15.4 wt% weightloss (organic)

Surface area: 434 m^2/g

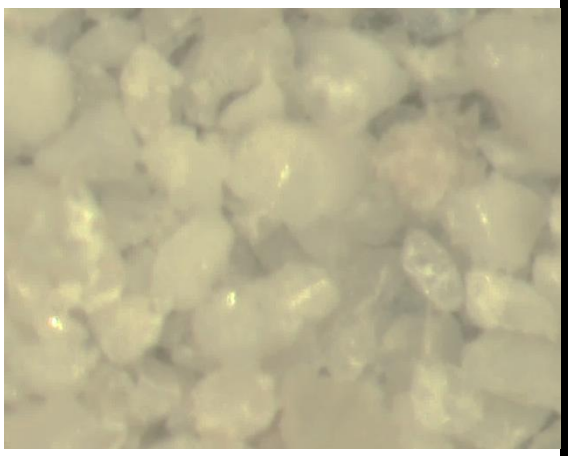

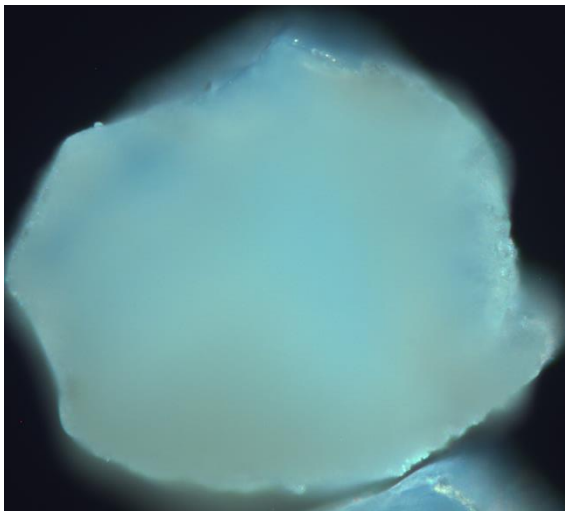

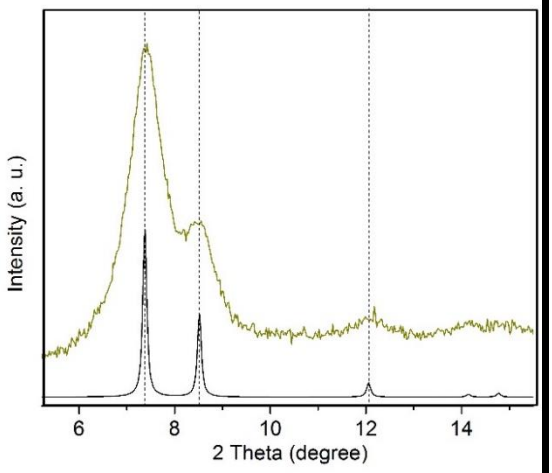

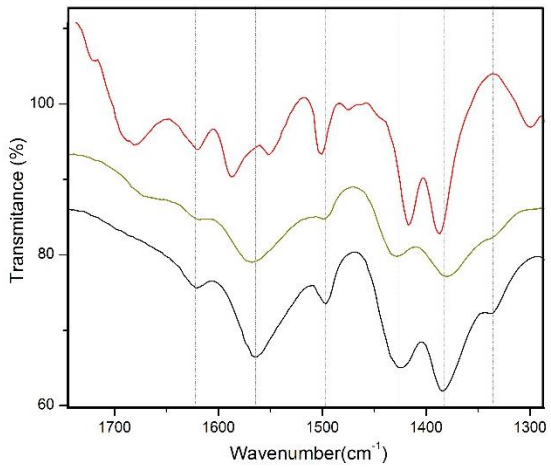

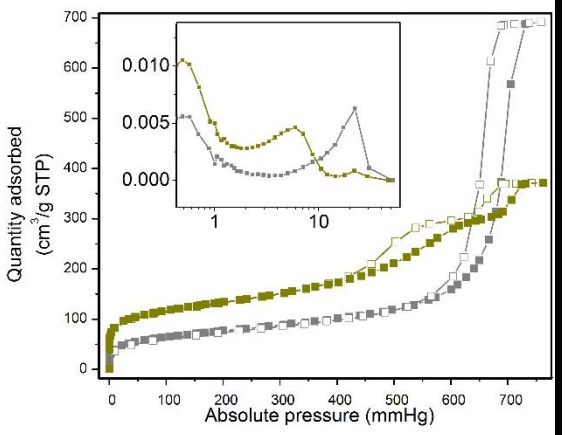

MDS F3a

(Zr)UiO-67(Bpy)/ Silica(A)

$Zr_6O_4(OH)_4(BpyDC)_6$ [MW=2140, 25.5 wt% Zr]

Ligand salt precursor solution*:*

2 mL of 150 mg *H_2BpyDC*+175 µL TEA/ mL H_2O

Metal salt precursor solution:

1.5 mL of 250 mg *$ZrOCl_2 \cdot 8H_2O$* / mL H_2O

Trace of solvent: 15 wt % H_2O

Synthesis conditions: 120 °C for 2 hours

XRF: 22.6% MOF (34.2 wt% max)

Yield = 66.0%

TGA: 14.0 wt% weightloss (organic)

Surface area: 366 m^2/g

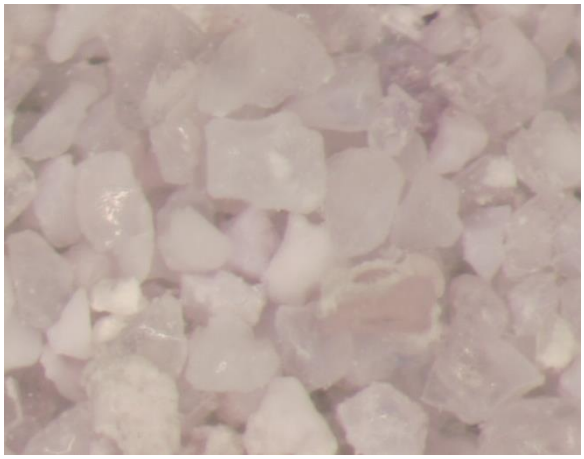

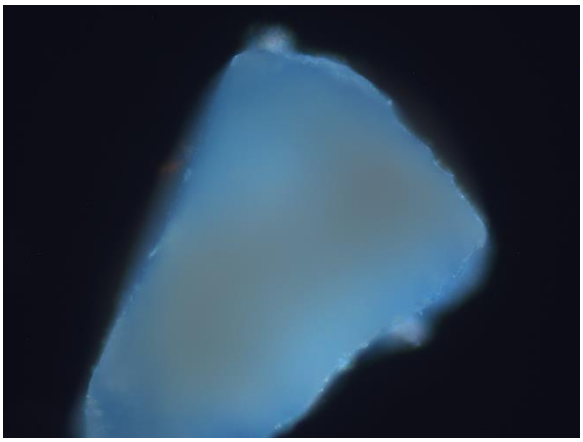

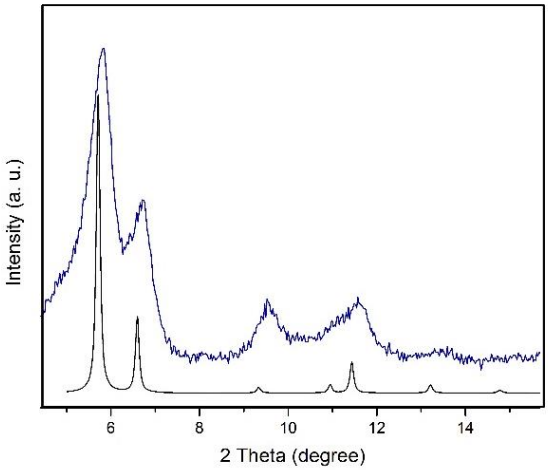

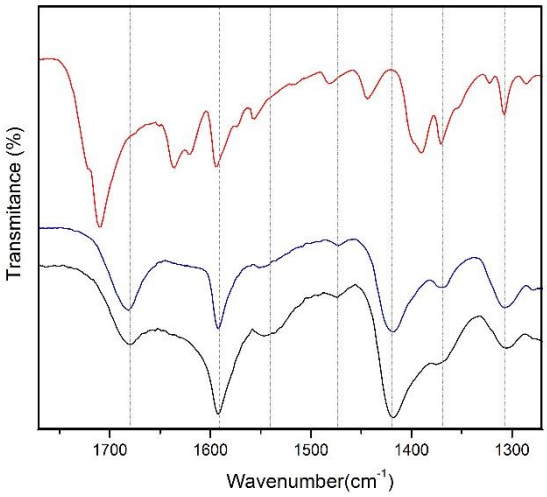

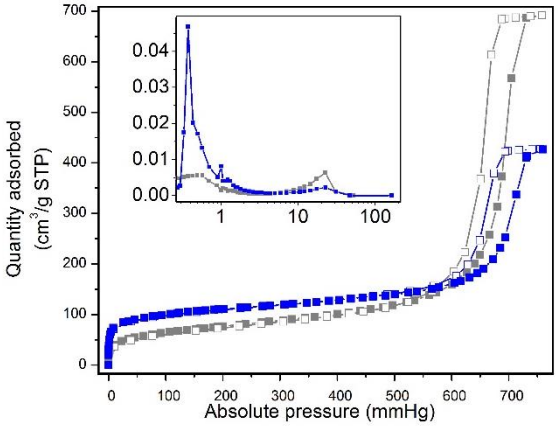

MDS G1a

(Zn)ZIF-8/ Silica(A)

$Zn(MeIM)_2 \cdot 2(H_2O)$ [MW = 227; 28.6 wt% Zn]

Metal salt precursor solution

2 mL of *240 mg $Zn(NO_3)_2 \cdot 6H_2O$* / mL H_2O[a]

Ligand salt precursor solution*:*

1.5 mL of 240 mg *HMeIM* / mL H_2O[b]

Trace of solvent: vapor of Et_3N

Synthesis conditions: RT for 1 hour

XRF: 34.1 wt% MOF (57.6 wt% max)

Yield = 59.2%

TGA = 21.5 wt% weightloss (organic)

Surface area: 346 m^2/g

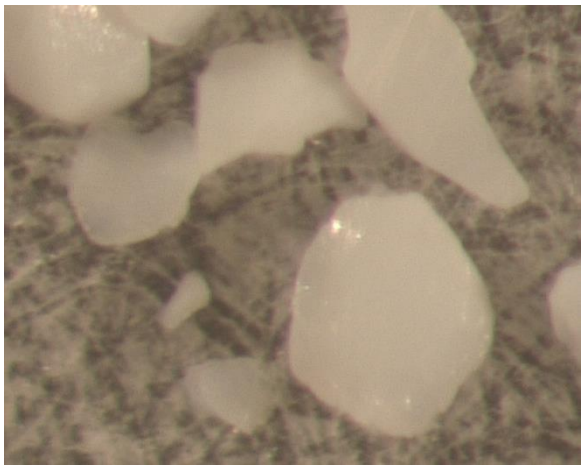

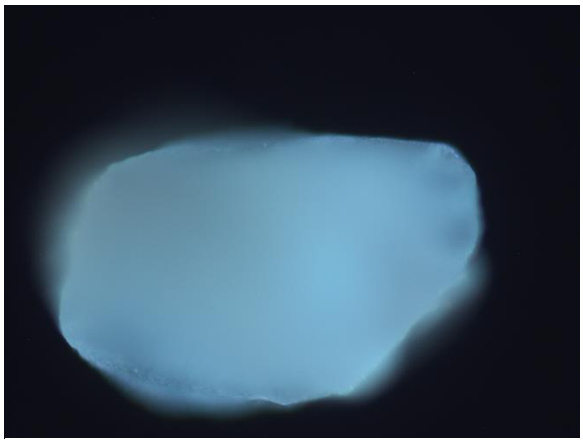

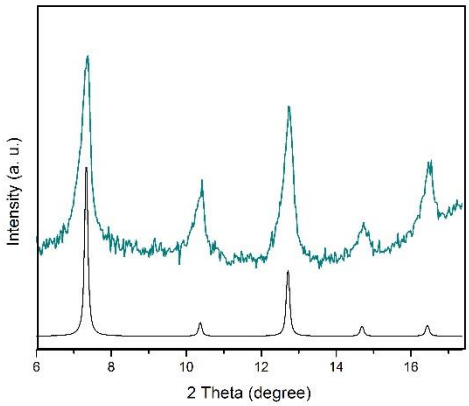

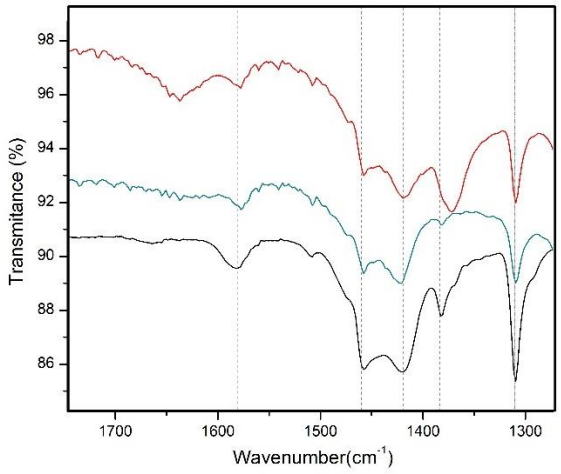

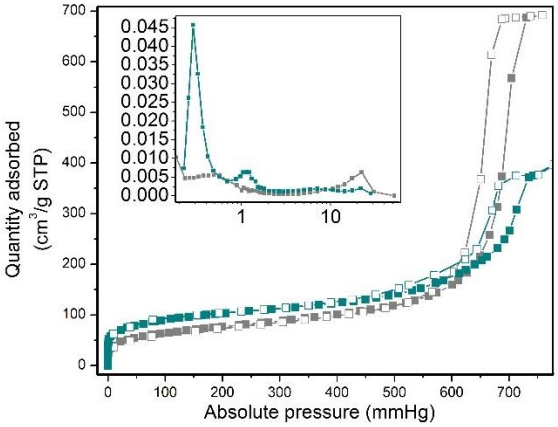

[a] Metal salt precursor is impregnated first for ZIF-8/MPM hybrid materials. [b] An acidification step is not required for ZIF-8/MPM hybrid materials.

MDS H1a

(Ru)HKUST-1/ Silica(A)

$Ru_3Cl_{1.5}(BTC)_2$*·1.5(AcOH)*

[MW = 857; 35.3 wt% Ru]

Ligand salt precursor solution*:*

2 mL of 75 mg *$Na_3(BTC)$* / mL H_2O

Metal salt precursor solution*:*

1.5 mL of 150 mg *$RuCl_3 \cdot xH_2O$* / 1 mL H_2O

Trace of solvent: 15 wt%H_2O

Synthesis conditions: 160 °C for 24 h

XRF: 11.0 wt% MOF (23.0 wt% max)

Yield = 47.8%

TGA = 8.0 wt% weightloss (organic)

Surface area: 258 m^2/g

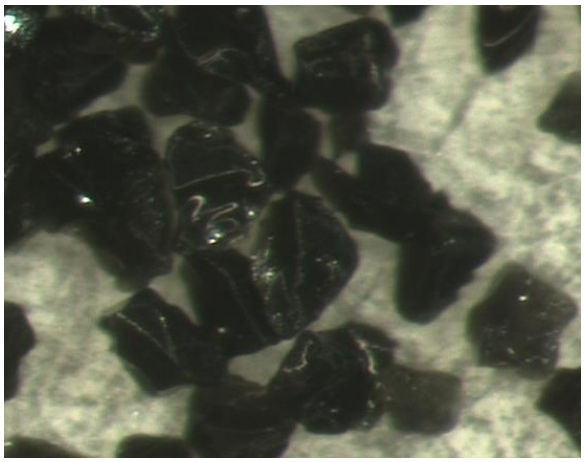

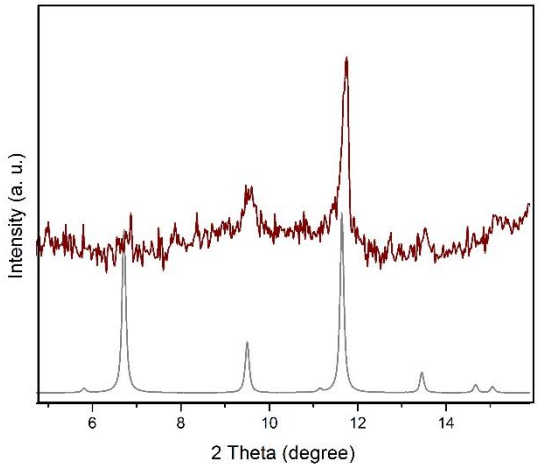

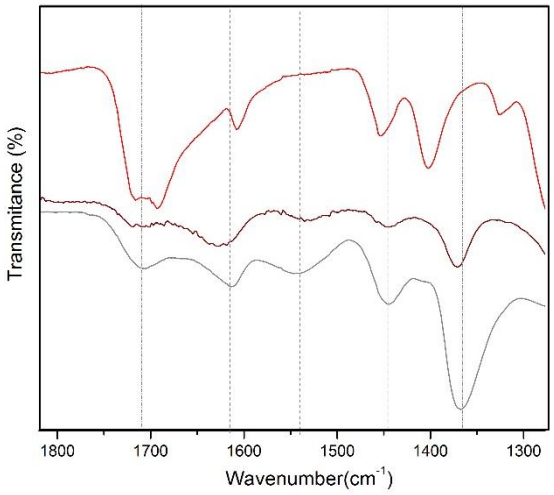

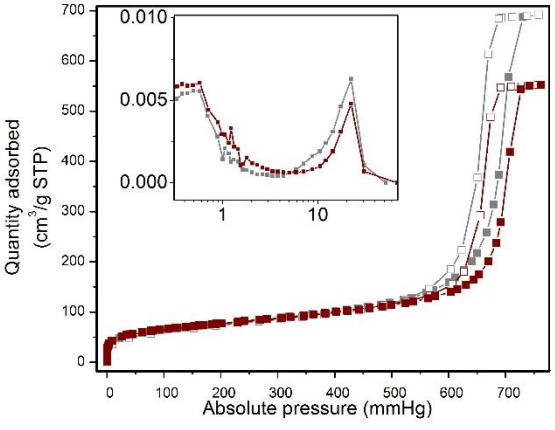

MDS-I1a: (Zr)PCN-222/ Silica(A)

$Zr_6(OH)_8(TCPP)_2$ (MW=2254, 26.2 wt% Zr)

Ligand salt precursor solution*:*

2 mL of 50 mg/mL H_4TCPP+40 µL TEA / mL H_2O

Metal salt precursor solution*:*

1.5 mL of 100 mg $ZrOCl_2 \cdot xH_2O$ / mL H_2O

Trace of solvent: 15 %wt DMF

Synthesis conditions: 120 °C for 12 hours

XRF: 9.8% MOF (14.6 wt% max)

Yield = 67.1 %

TGA: 7.2 wt% weightloss (organic)

Surface area: 348 m^2/g

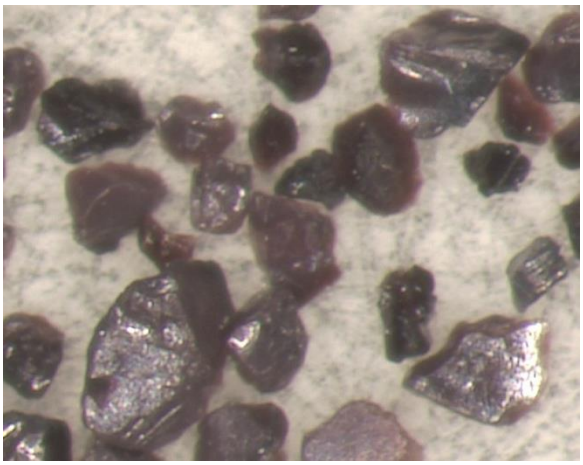

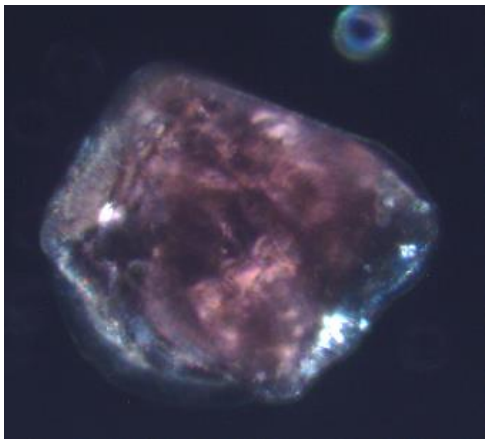

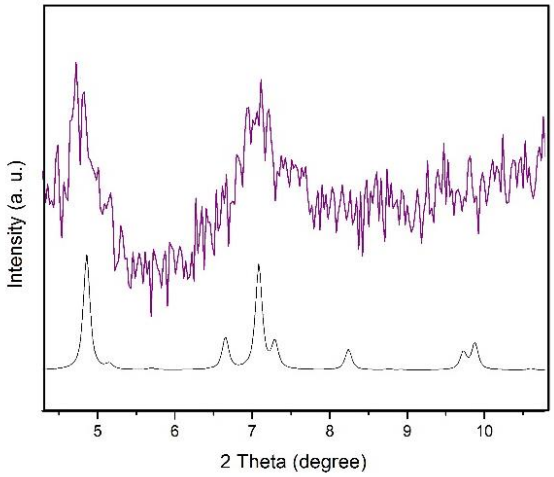

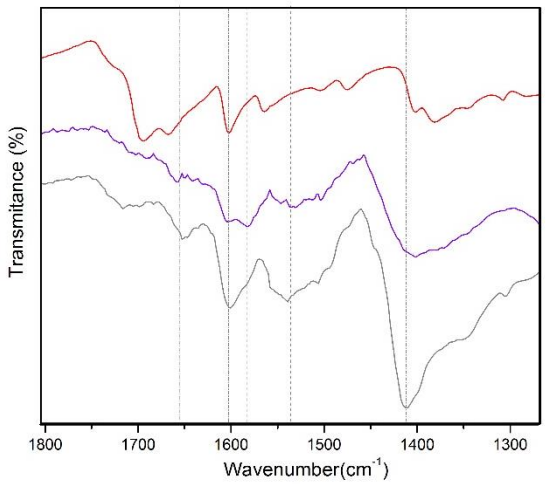

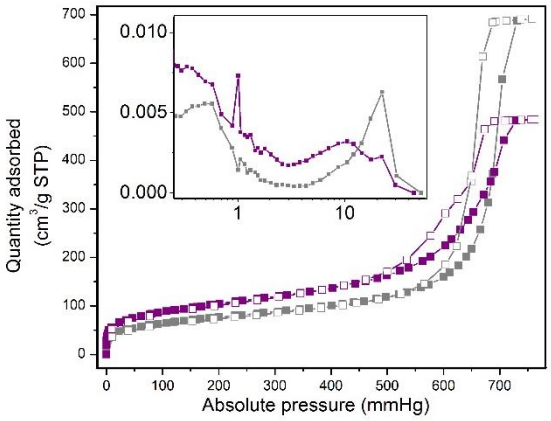

MDS J1a
(Zr)NU-1000/ Silica(A)
$Zr_6(OH)_8(TBAPy)_2$ (MW=2038, 26.7 wt% Zr)
Ligand salt precursor solution*:*
2 mL of 50 mg *H_4TBAPy* + 40 µL TEA / mL H_2O
Metal salt precursor solution:
1.5 mL 100 mg *$ZrOCl_2 \cdot xH_2O$* / mL H_2O
Trace of solvent: 15 %wt DMF
Synthesis conditions: 120 °C for 12 hours
XRF: 12.8 % MOF (15.0 wt% max)
Yield = 85.5 %
TGA = 9.6 wt%
Surface area: 364 m^2/g

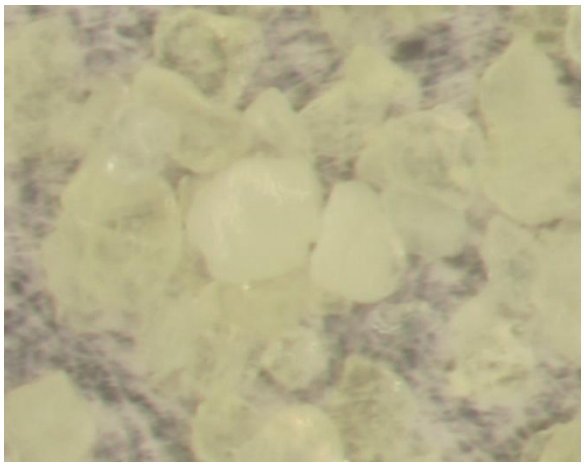

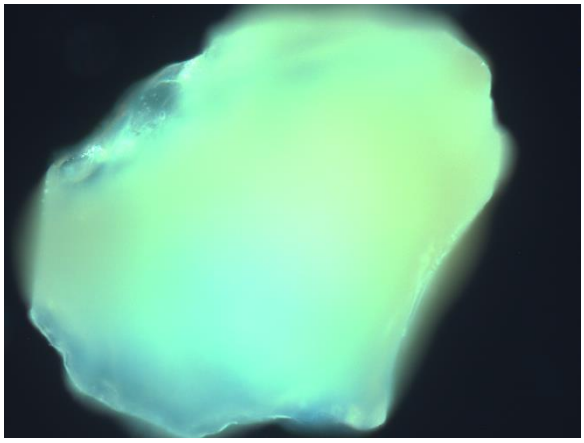

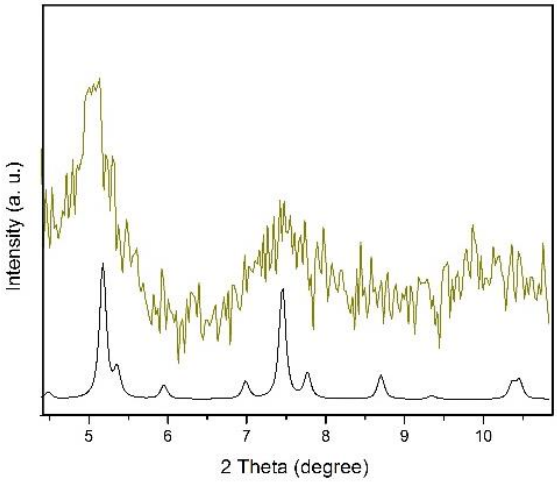

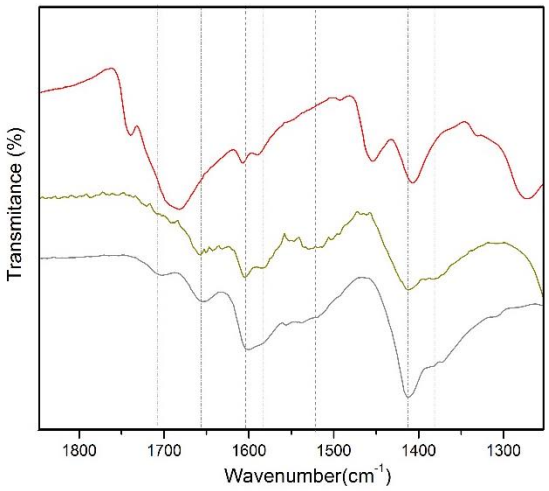

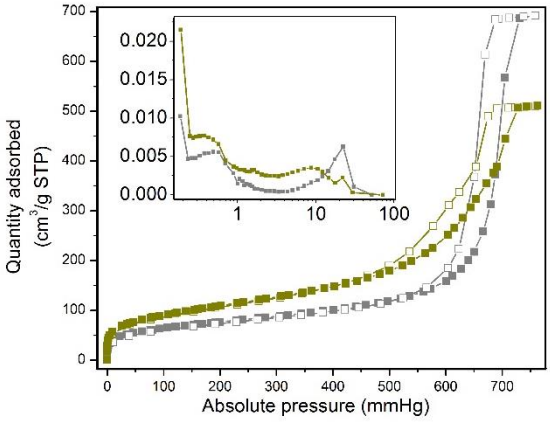

[a] Material was additionally washed using HCl 1M in DMF at 100 °C for 24 hours, as reported for pure NU-1000.

MDS K1a

Co_2(DOBPDC)/ Silica(A)

$Co_2(DOBPDC)\cdot 2(H_2O)_2$ [MW=429; 27.5 wt% Co]

Ligand salt precursor solution*:*

2 mL of 75 mg *$H_4DOBPDC$*+40 µL TEA / mL H_2O

Metal salt precursor solution*:*

1.5 mL of 200 mg *$Co(NO_3)_2\cdot 6H_2O$* / mL H_2O

Trace of solvent: vapor of Et_3N

Synthesis conditions: RT for 1 hours

XRF: 13.4 wt% MOF (23.4 wt% max)

Yield = 57.2%

TGA = 8.3 wt% weightloss (organic)

Surface area: 344 m^2/g

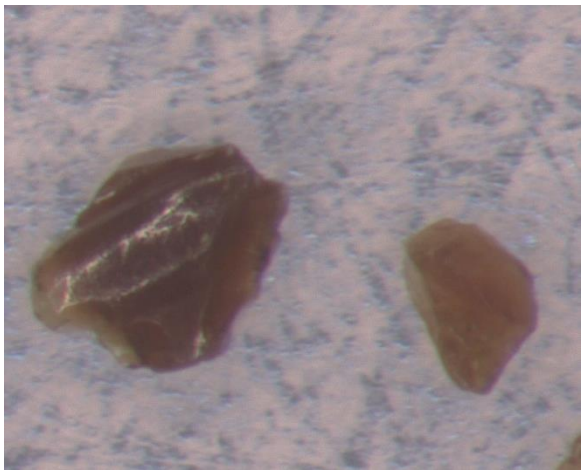

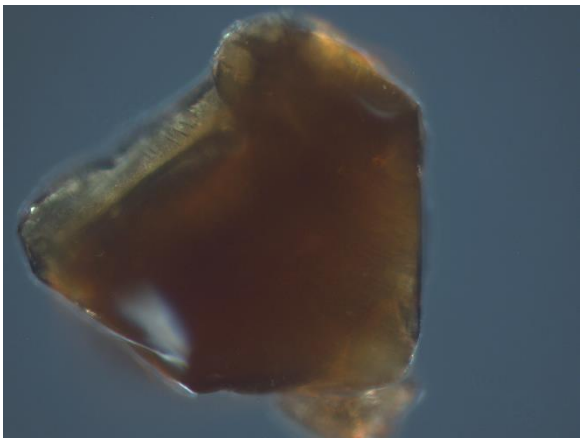

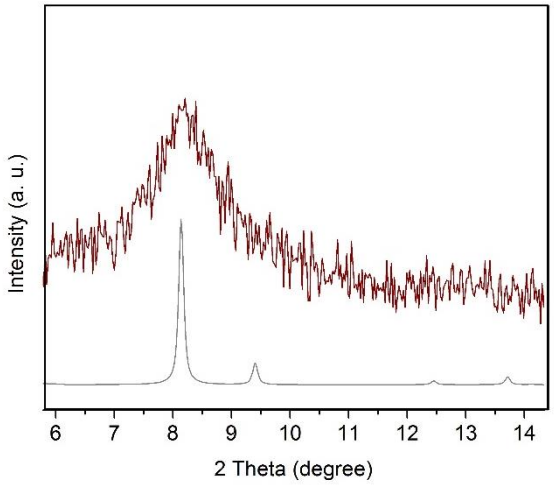

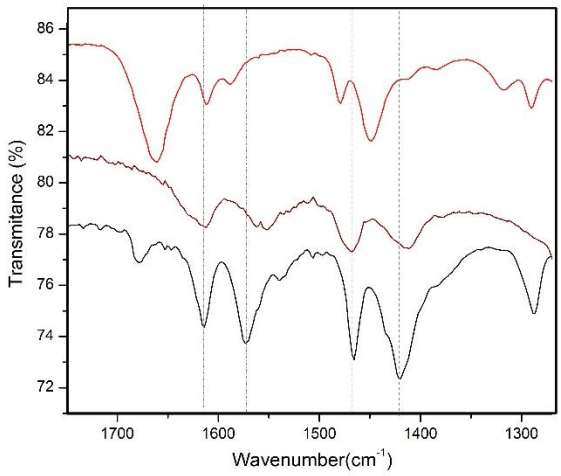

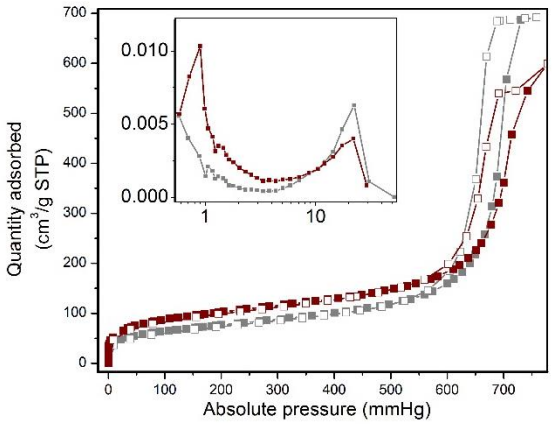

MDS A2a

(Cr)MIL-101(SO_3H)/Silica(A)

$Cr_3O(OH)(BDC\text{-}SO_3H)_3 \cdot 2H_2O$

[MW = 957; 16.3 wt% Cr]

Ligand salt precursor solution*:*

2 mL of 200 mg *$H_2BDC(SO_3Na)$* / mL H_2O

Metal salt precursor solution*:*

1.5 mL of 200 mg *$Cr(NO_3)_3 \cdot 9H_2O$* / mL H_2O

Trace of solvent: 15 wt% H_2O

Synthesis conditions: 190 °C for 24 h

XRF: 19.1 wt% MOF (23.9% wt% max.)

Yield = 79.9%

TGA: 13.3 wt% weight loss (organic)

Surface area: 486 m^2/g

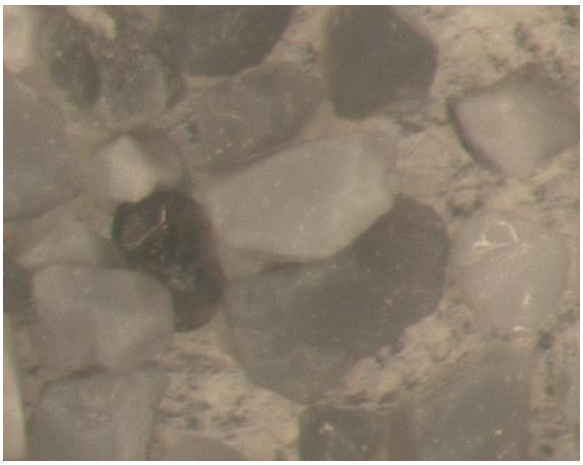

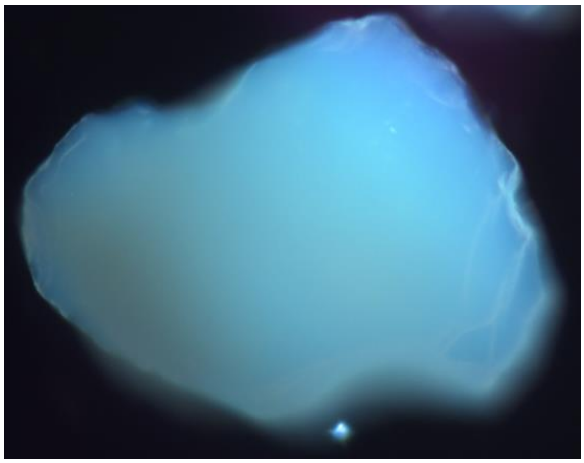

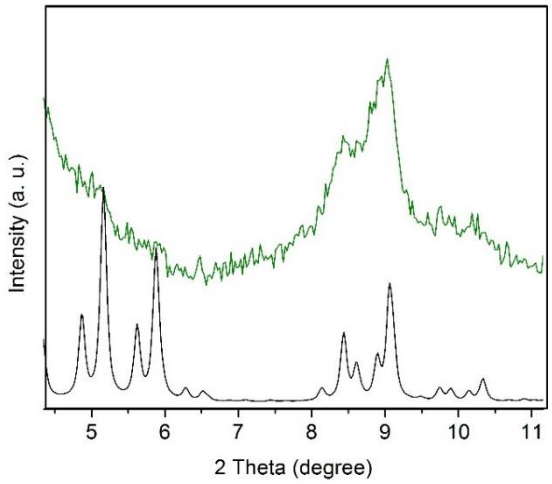

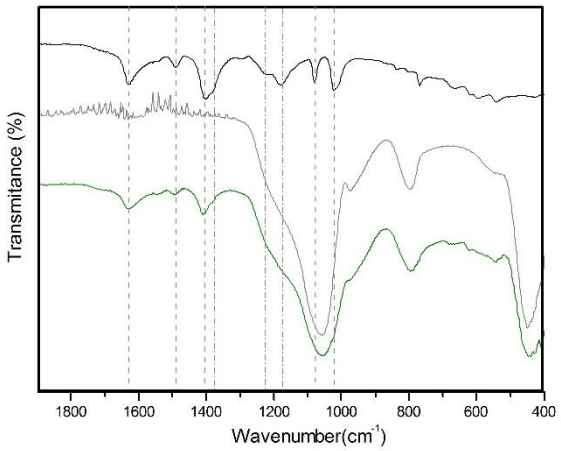

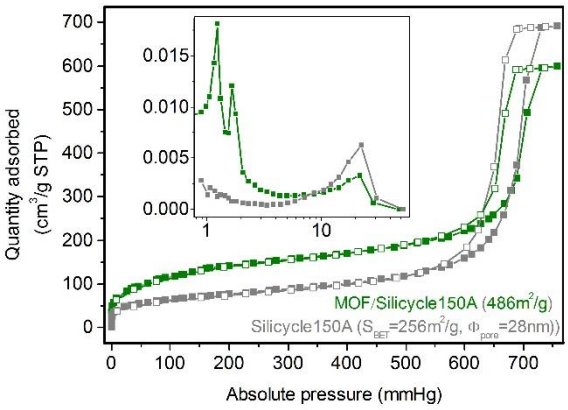

**40. 8 wt% (Cr)MIL-101(SO_3H)/Silica(A) is obtained via second solid-state crystallization on 19.1 wt% (Cr)MIL-101(SO_3H)/Silica(A).*

MDS A2b

(Cr)MIL-101(SO_3H)/Silica(B)

$Cr_3O(OH)(BDC\text{-}SO_3H)_3 \cdot 2H_2O$

[MW = 957; 16.3 wt% Cr]

Ligand salt precursor solution*:*

2 mL of 200 mg *$H_2BDC(SO_3Na)$* / mL H_2O

Metal salt precursor solution*:*

1.5 mL of 200 mg *$Cr(NO_3)_3 \cdot 9H_2O$* / mL H_2O

Trace of solvent: 15 wt% H_2O

Synthesis conditions: 190 °C for 24 h

XRF: 21.9 wt% MOF (23.9% wt% max.)

Yield = 91.6 %

TGA: 14.1 wt% weight loss (organic)

Surface area: 577 m^2/g

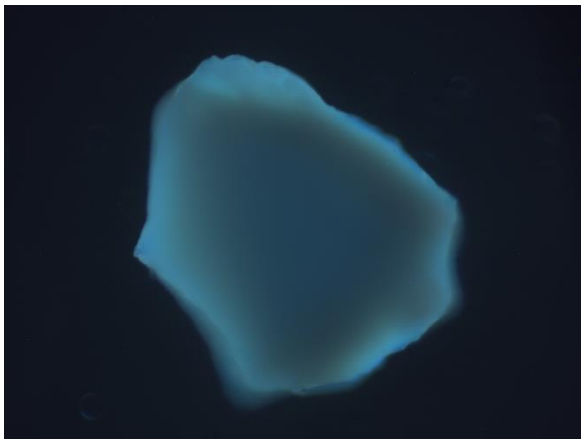

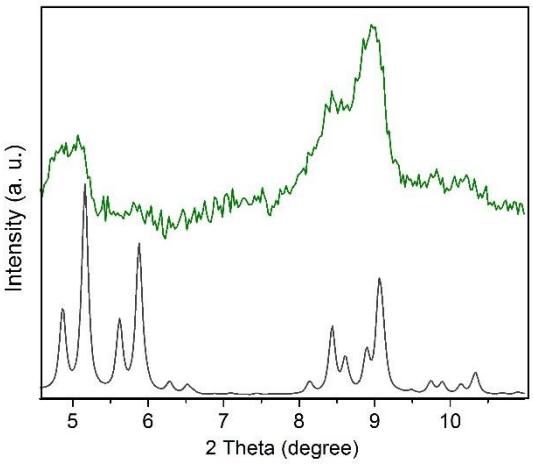

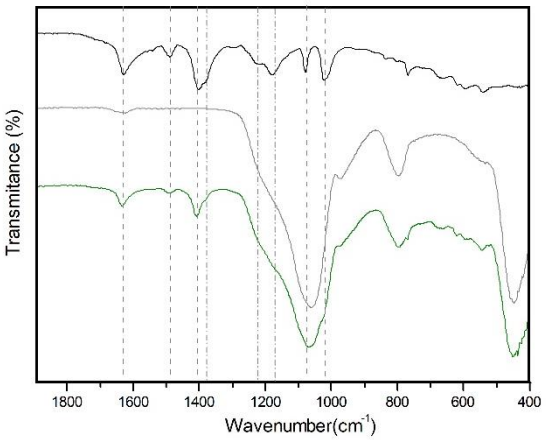

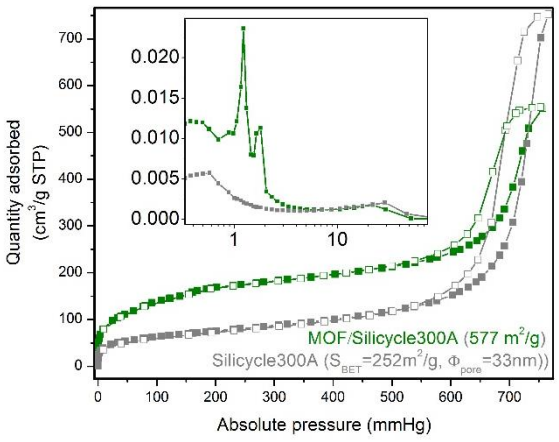

MDS A2c

(Cr)MIL-101(SO_3H)/Silica(C)

$Cr_3O(OH)(BDC\text{-}SO_3H)_3 \cdot 2H_2O$

[MW = 957; 16.3 wt% Cr]

Ligand salt precursor solution*:*

1.8 mL of 200 mg *$H_2BDC(SO_3Na)$* / mL H_2O

Metal salt precursor solution*:*

1.4 mL of 200 mg *$Cr(NO_3)_3 \cdot 9H_2O$* / 1 mL H_2O

Trace of solvent: 15 wt% H_2O

Synthesis conditions: 190 °C for 24 h

XRF: 17.7 wt% MOF (22.3% wt% max.)

Yield = 79.3%

TGA: 8.3 wt% weight loss (organic)

Surface area: 320 m^2/g

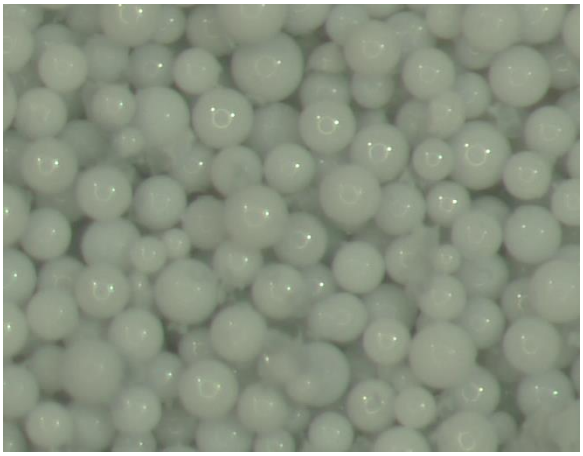

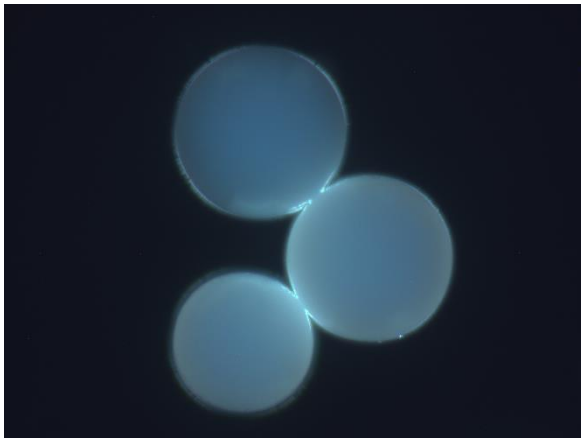

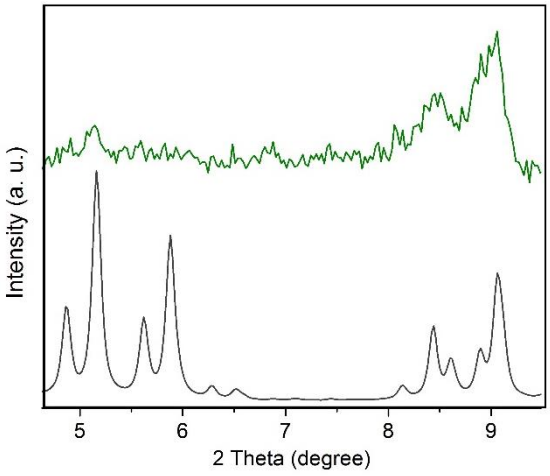

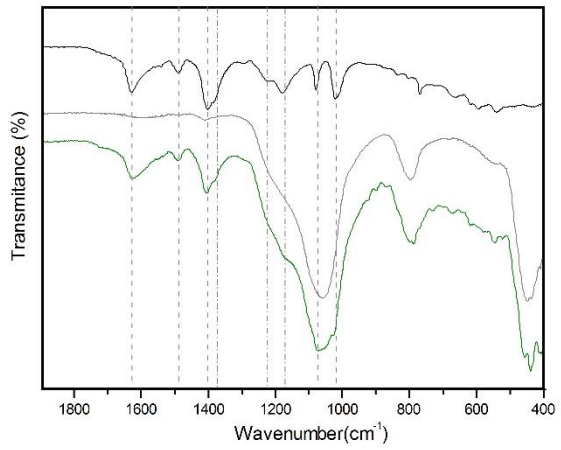

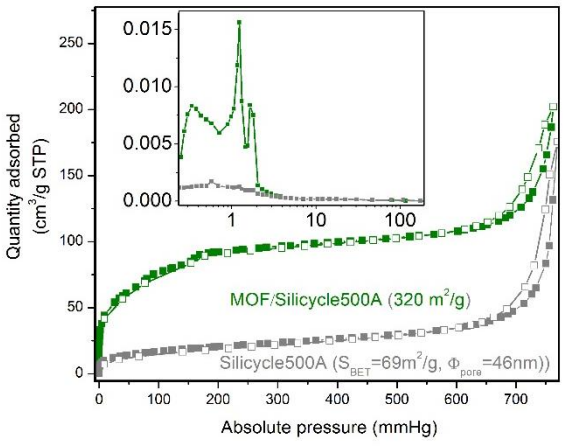

MDS A2d

(Cr)MIL-101(SO_3H)/Silica(D)

$Cr_3O(OH)(BDC\text{-}SO_3H)_3 \cdot 2H_2O$

[MW = 957; 16.3 wt% Cr]

Ligand salt precursor solution*:*

1.8 mL 200 mg *$H_2BDC(SO_3Na)$* / 1 mL H_2O

Metal salt precursor solution*:*

1.4 mL 200 mg *$Cr(NO_3)_3 \cdot 9H_2O$* / 1 mL H_2O

Trace of solvent: 15 wt% H_2O

Synthesis conditions: 190 °C for 24 h

XRF: 14.3 wt% MOF (22.3% wt% max.)

Yield = 64.1%

TGA: 9.4 wt% weight loss (organic)

Surface area: 373 m^2/g

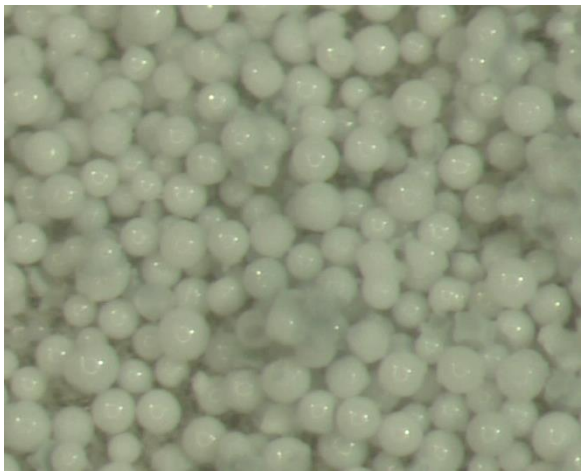

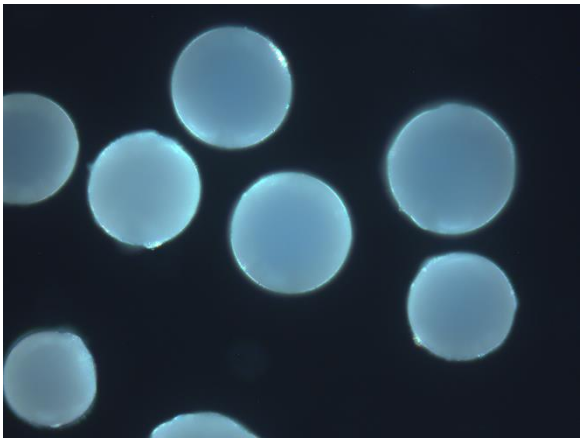

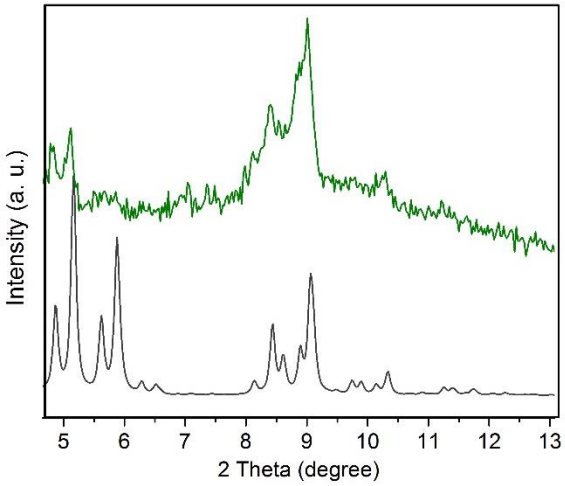

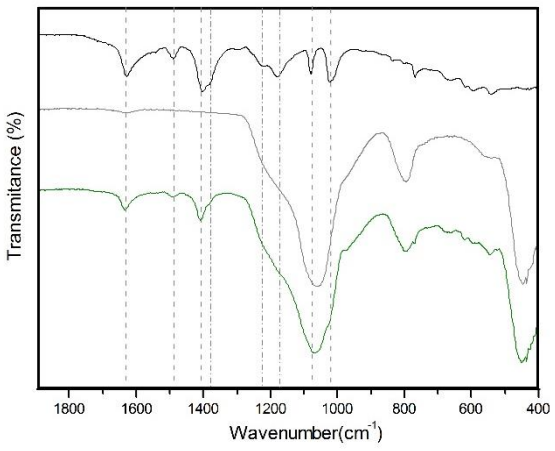

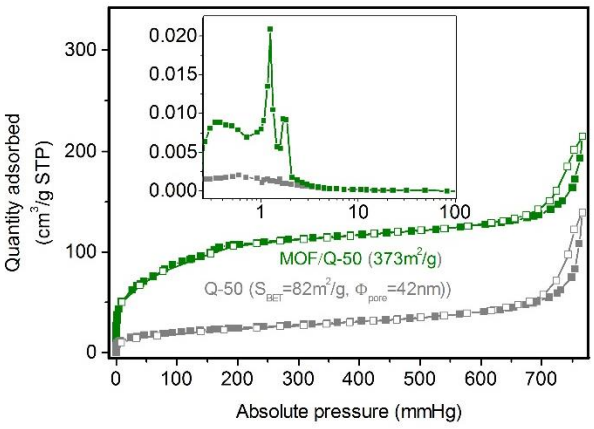

MDS A2e

(Cr)MIL-101(SO_3H)/SBA-15

$Cr_3O(OH)(BDC\text{-}SO_3H)_3 \cdot 2H_2O$

[MW = 957; 16.3 wt% Cr]

Ligand salt precursor solution*:*

3.5 mL 200 mg *$H_2BDC(SO_3Na)$* / mL H_2O

Metal salt precursor solution*:*

3 mL of 200 mg *$Cr(NO_3)_3 \cdot 9H_2O$* / mL H_2O

Trace of solvent: 15 wt% H_2O

Synthesis conditions: 190 °C for 24 h

XRF: 21.9 wt% MOF (47.8% wt% max.)

Yield = 45.8%

TGA: 16.5 wt% weight loss (organic)

Surface area: 786 m^2/g

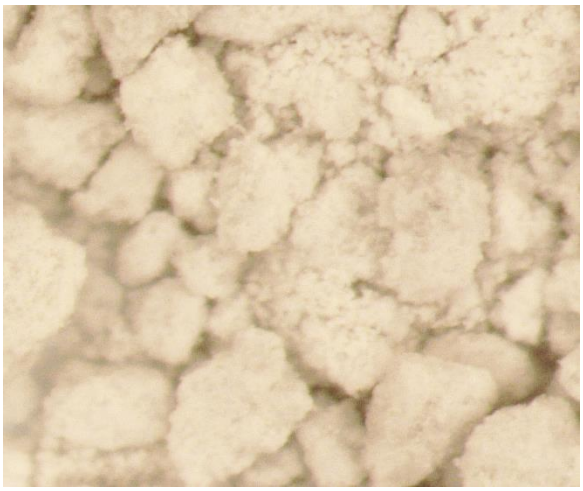

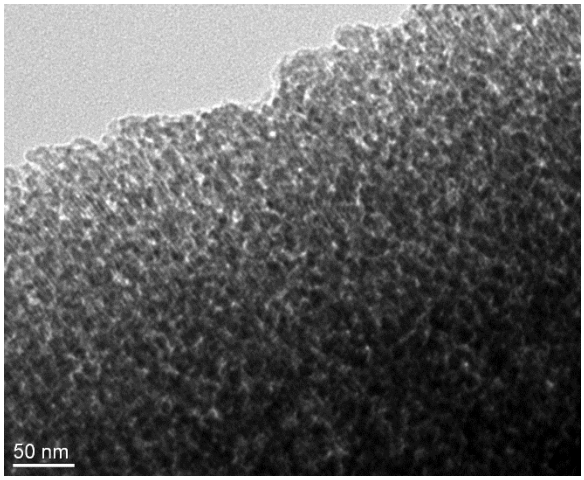

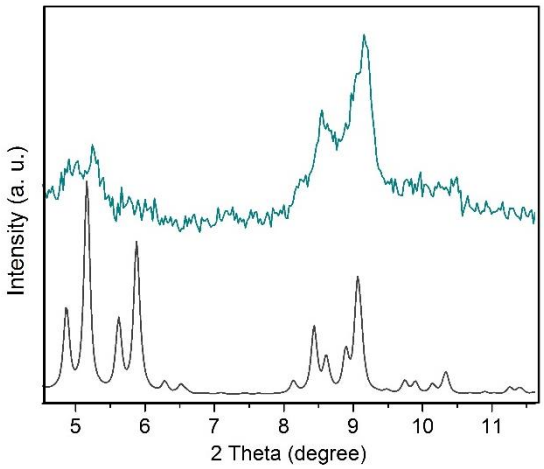

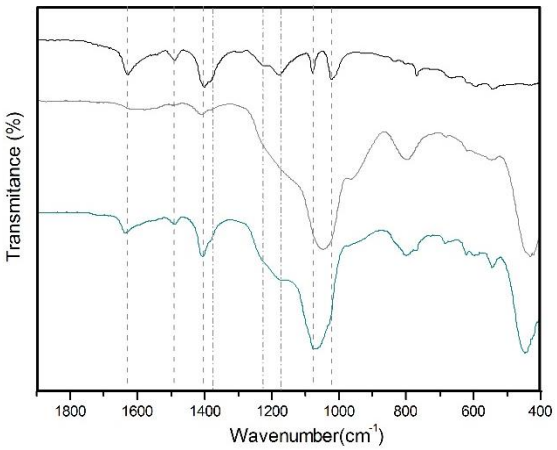

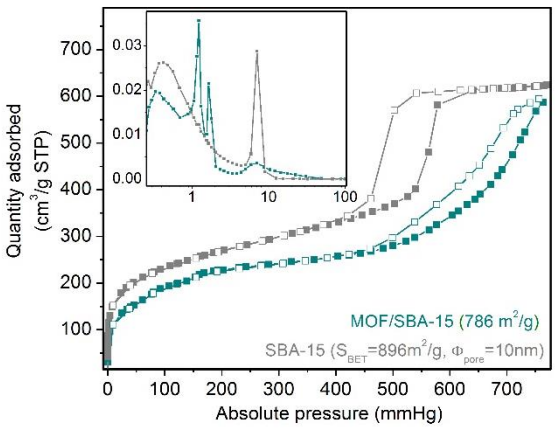

MDS A2f

(Cr)MIL-101(SO_3H)/MCM-41

$Cr_3O(OH)(BDC\text{-}SO_3H)_3 \cdot 2H_2O$

[MW = 957; 16.3 wt% Cr]

Ligand salt precursor solution*:*

3.5 mL 200 mg *$H_2BDC(SO_3Na)$* / mL H_2O

Metal salt precursor solution*:*

3 mL of 200 mg *$Cr(NO_3)_3 \cdot 9H_2O$* / mL H_2O

Trace of solvent: 15 wt% H_2O

Synthesis conditions: 190 °C for 24 h

XRF: 21.9 wt% MOF (47.8% wt% max.)

Yield = 45.8%

TGA: 11.3 wt% weight loss (organic)

Surface area: 172m^2/g

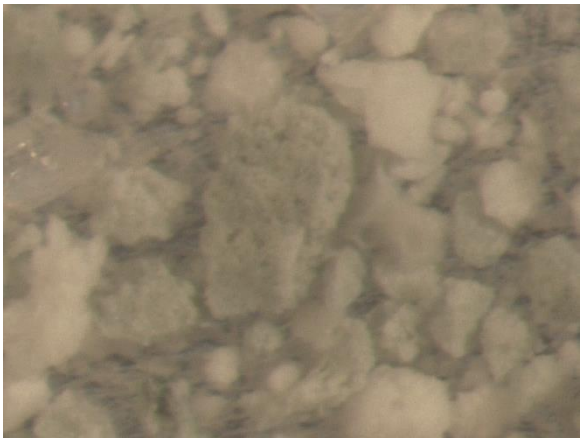

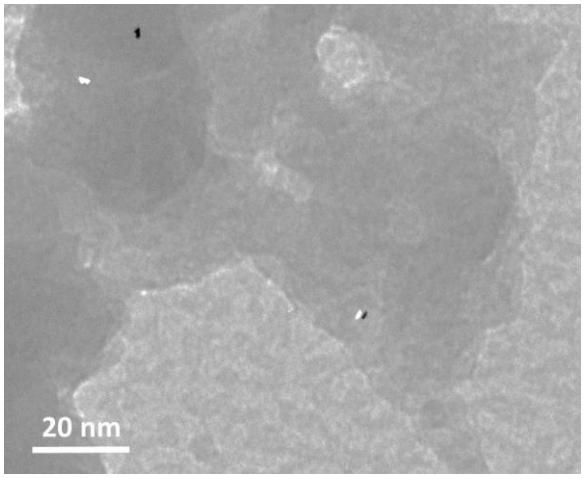

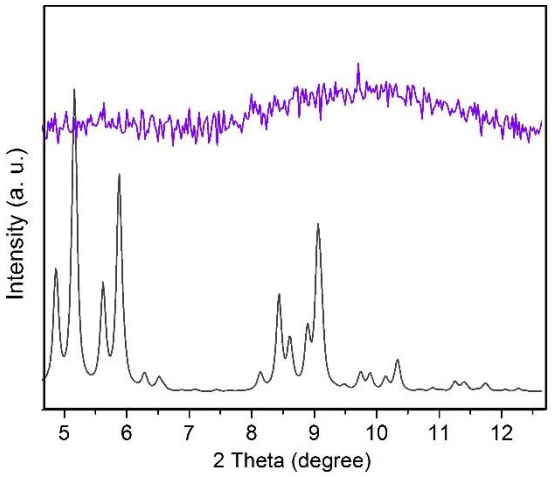

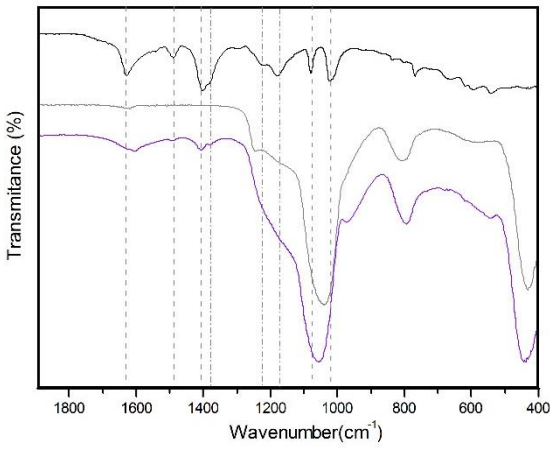

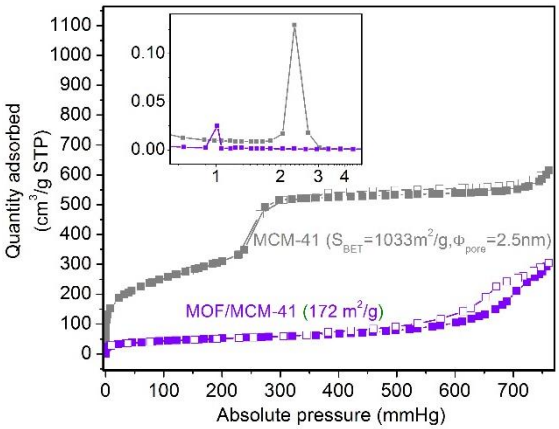

MDS A2g

(Cr)MIL-101(SO_3H)/Carbon

$Cr_3O(OH)(BDC\text{-}SO_3H)_3 \cdot 2H_2O$

[MW = 957; 16.3 wt% Cr]

Ligand salt precursor solution*:*

1.5 mL of 200 mg *$H_2BDC(SO_3Na)$* / mL H_2O

Metal salt precursor solution*:*

1.2 mL of 200 mg *$Cr(NO_3)_3 \cdot 9H_2O$* / mL H_2O

Trace of solvent: 25 wt% H_2O

Synthesis conditions: 190 °C for 24 h

XRF: 13.3 wt% MOF (19.1% wt% max.)

Yield = 69.6%

TGA: 9.1 wt% weight loss (inorganic)[a]

Surface area: 406 m^2/g

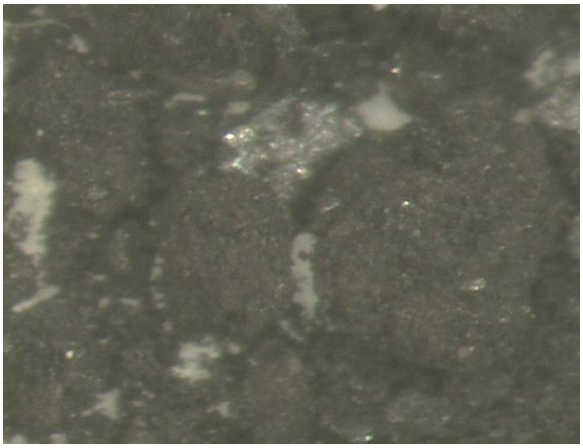

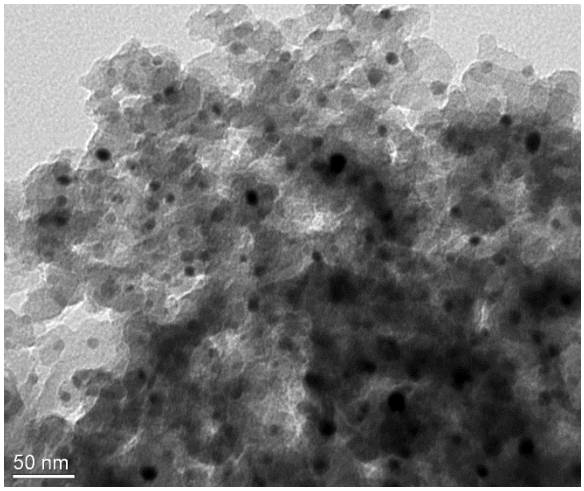

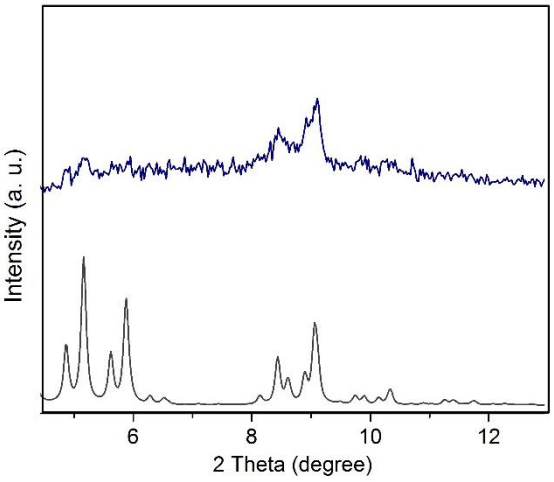

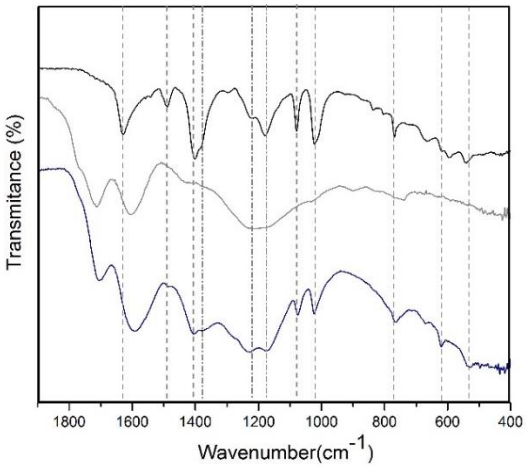

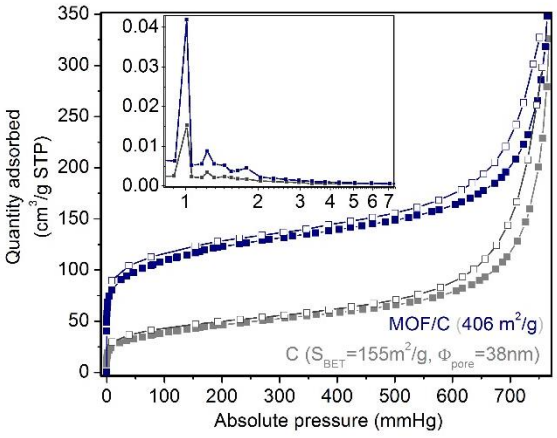

[a] *Calculated amount of inorganic component after the decomposition of the sample at 1000 °C under air corresponding to remaining Cr_2O_3, since the mesoporous material is purely organic.*

MDS A2h

(Cr)MIL-101(SO_3H)/γ-Al_2O_3

$Cr_3O(OH)(BDC\text{-}SO_3H)_3 \cdot 2H_2O$

[MW = 957; 16.3 wt% Cr]

Ligand salt precursor solution*:*

1.5 mL of 200 mg *$H_2BDC(SO_3Na)$* / mL H_2O

Metal salt precursor solution*:*

1.2 mL of 200 mg *$Cr(NO_3)_3 \cdot 9H_2O$* / mL H_2O

Trace of solvent: 25 wt% H_2O

Synthesis conditions: 190 °C for 24 h

XRF: 16.3 wt% MOF (19.1% wt% max.)

Yield = 85.3%

TGA: 20.0 wt% weight loss (organic) [a]

Surface area: 168 m^2/g

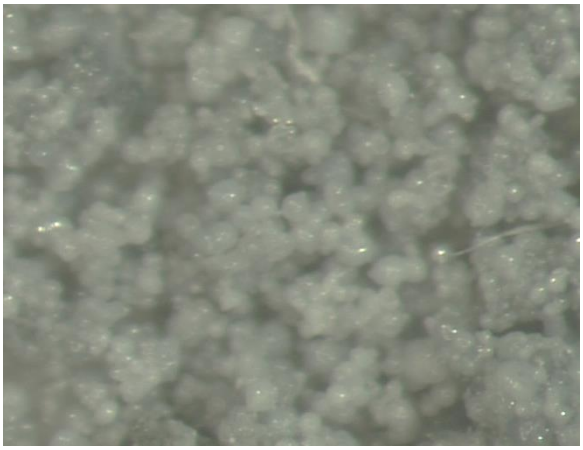

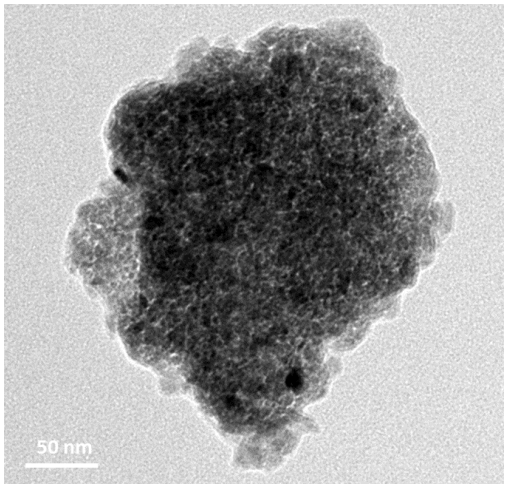

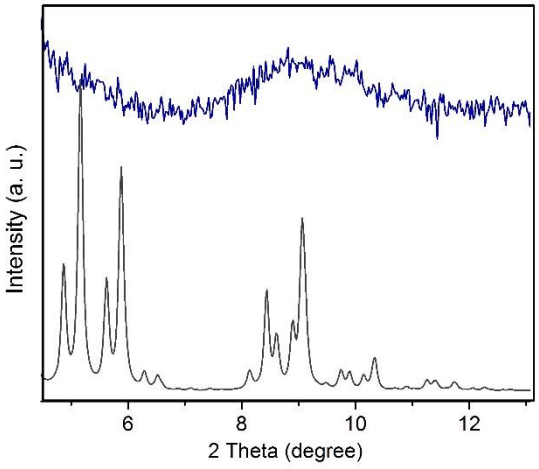

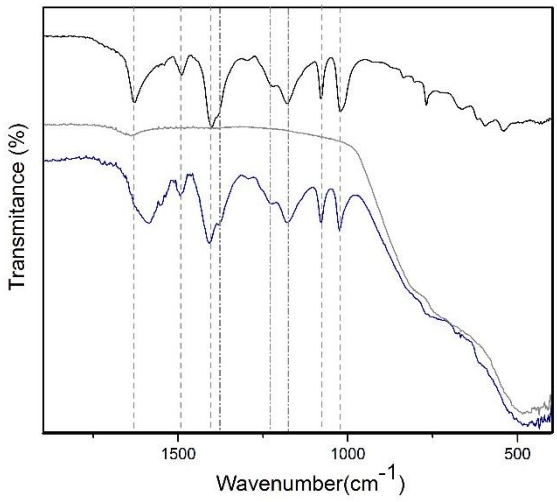

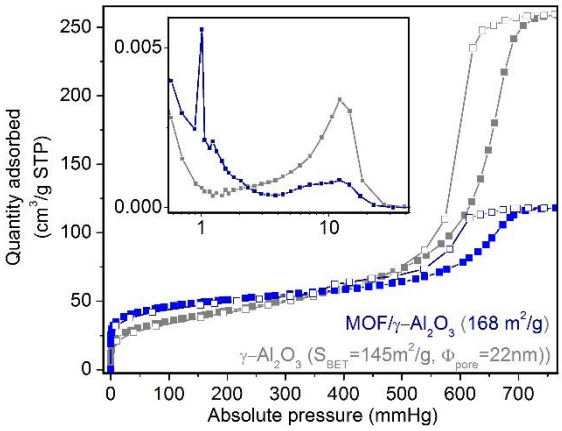

[a] *weightloss of organic is superior to MOF loading according to TGA due to either the formation of Al-containing coordination polymer or an excess amount of ligand is strongly bonded to the alumina surface.*

MDS A2i

(Cr)MIL-101(SO_3H)/ **TiO_2**

$Cr_3O(OH)(BDC\text{-}SO_3H)_3 \cdot 2H_2O$

[MW = 957; 16.3 wt% Cr]

Ligand salt precursor solution*:*

1.2 mL of 200 mg *$H_2BDC(SO_3Na)$* / mL H_2O

Metal salt precursor solution*:*

1.0 mL of 200 mg *$Cr(NO_3)_3 \cdot 9H_2O$* / mL H_2O

Trace of solvent: 25 wt% H_2O

Synthesis conditions: 190 °C for 24 h

XRF: 13.0 wt% MOF (19.5% wt% max.)

Yield = 56.7%

TGA: 18.9 wt% weight loss (organic)[a]

Surface area: 278 m^2/g

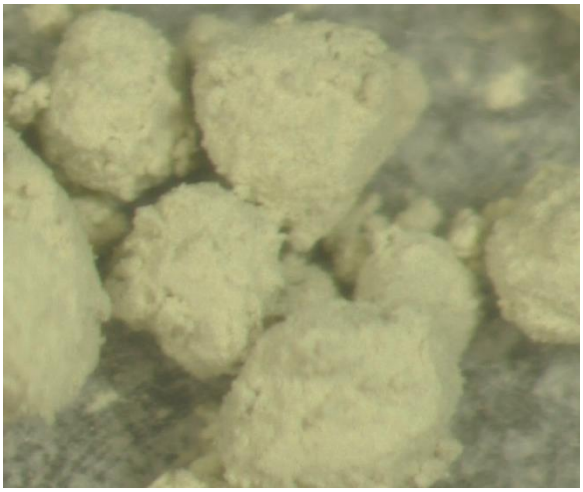

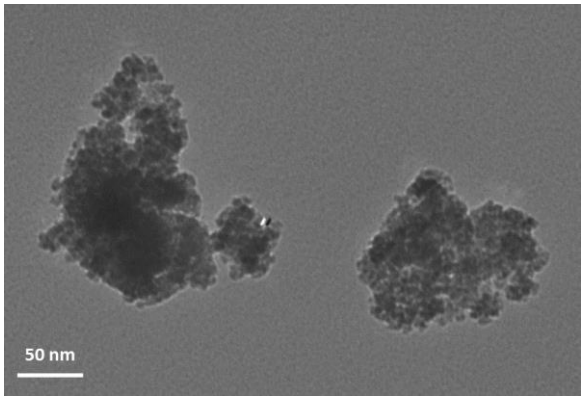

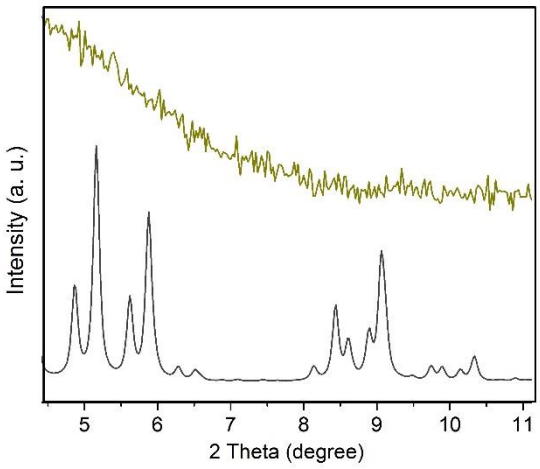

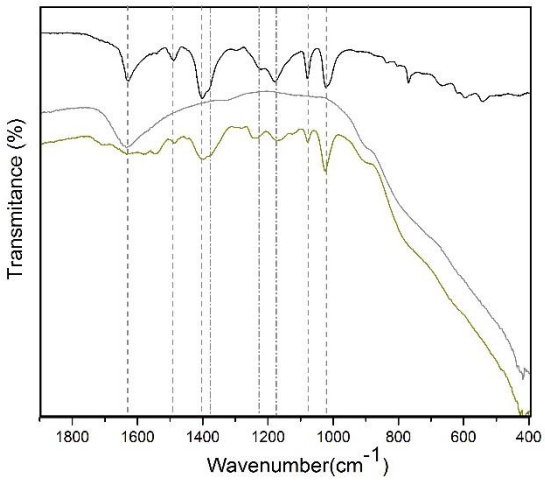

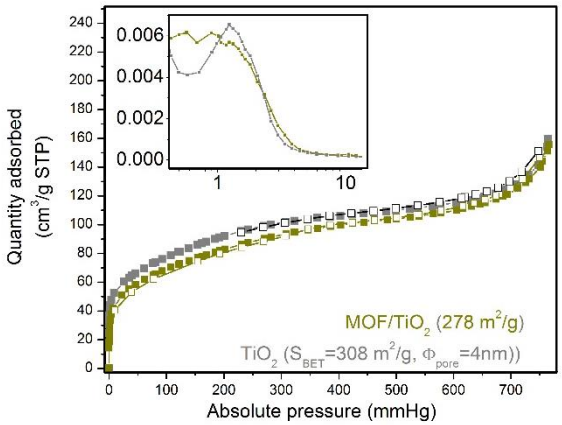

[a] *weightloss of organic is superior to MOF loading according to TGA due to either the formation of Ti-containing coordination polymer or an excess amount of ligand is strongly bonded to the titania surface.*

MDS A2j

(Cr)MIL-101(SO_3H)/ZrO_2

$Cr_3O(OH)(BDC\text{-}SO_3H)_3 \cdot 2H_2O$

[MW = 957; 16.3 wt% Cr]

Ligand salt precursor solution*:*

1.2 mL of 200 mg *$H_2BDC(SO_3Na)$* / mL H_2O

Metal salt precursor solution*:*

1.0 mL of 200 mg *$Cr(NO_3)_3 \cdot 9H_2O$* / mL H_2O

Trace of solvent: 25 wt% H_2O

Synthesis conditions: 190 °C for 24 h

XRF: 14.4 wt% MOF (19.5% wt% max.)

Yield = 73.8%

TGA: 8.36 wt% weight loss (organic)

Surface area: 142 m^2/g

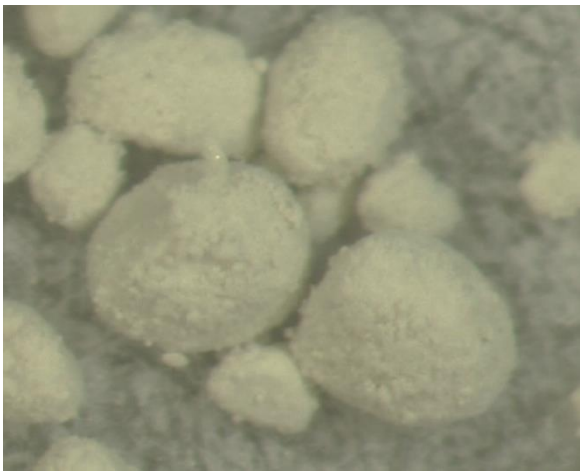

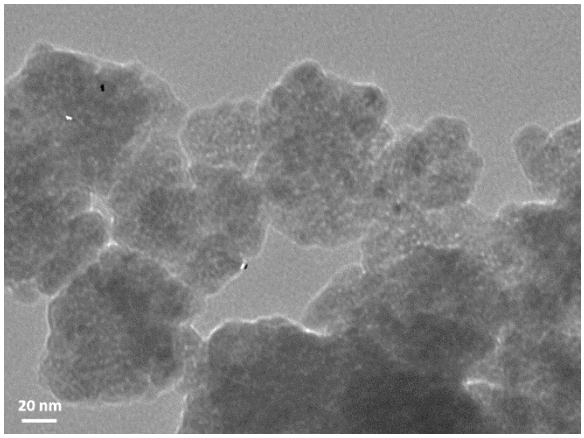

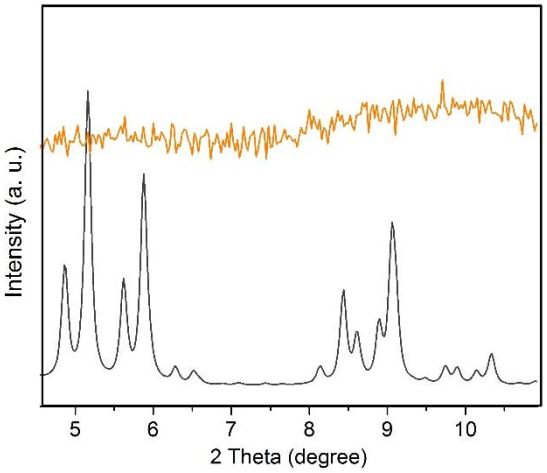

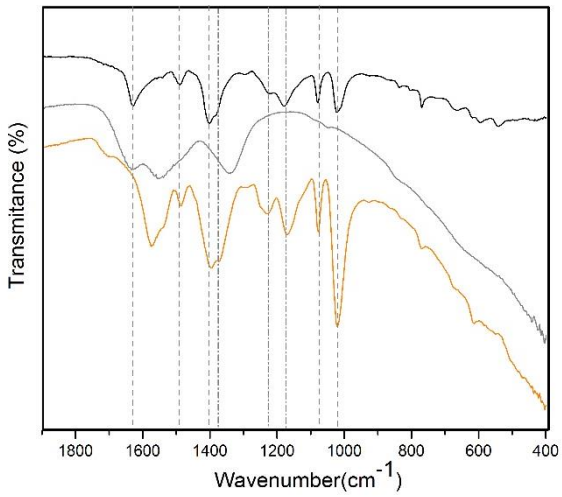

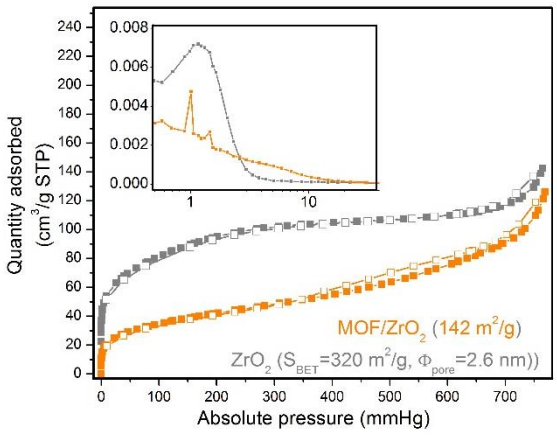

MDS A2k
(Cr)MIL-101(SO_3H)/HayeSep A
$Cr_3O(OH)(BDC\text{-}SO_3H)_3 \cdot 2H_2O$
[MW = 957; 16.3 wt% Cr]
Ligand salt precursor solution*:*
1.5 mL of 200 mg *$H_2BDC(SO_3Na)$* / mL H_2O
Metal salt precursor solution*:*
1.2 mL of 200 mg *$Cr(NO_3)_3 \cdot 9H_2O$* / mL H_2O
Trace of solvent: 25 wt% H_2O
Synthesis conditions: 190 °C for 24 h
XRF: 12.2 wt% MOF (19.1% wt% max.)
Yield = 63.8%
TGA: 3.8 wt% weight loss (inorganic)[a]
Surface area: 364 m^2/g

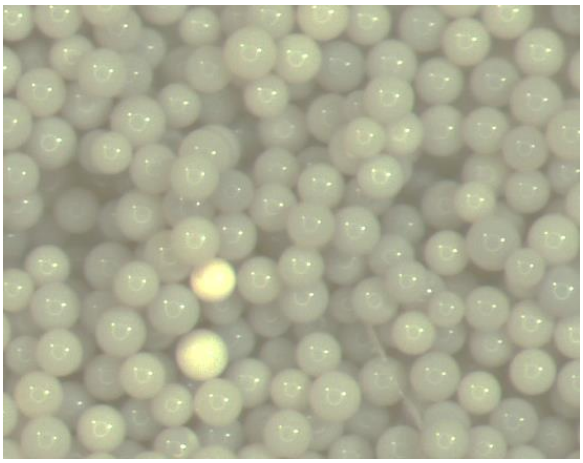

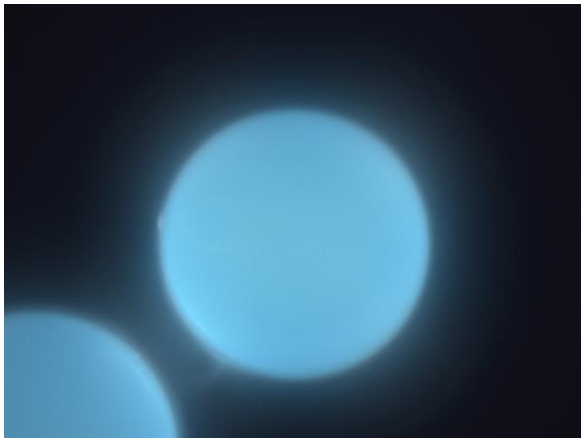

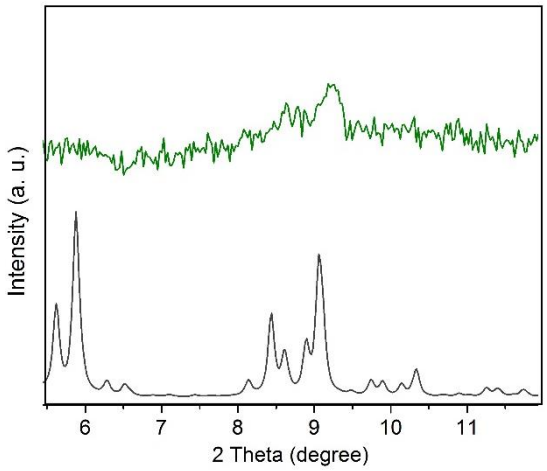

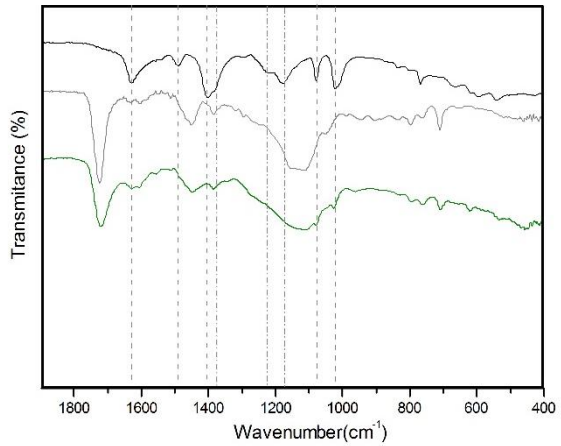

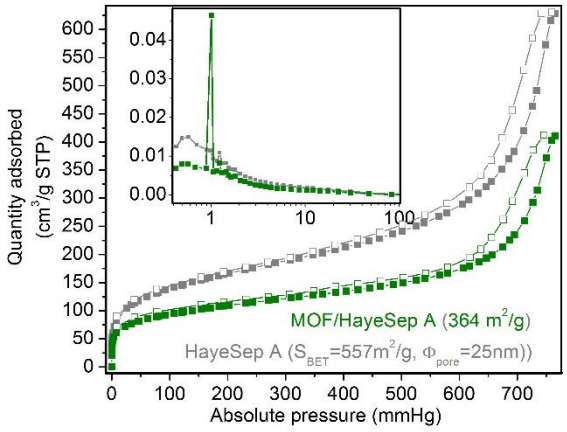

[a] *Calculated amount of inorganic component after the decomposition of the sample at 1000 °C under air corresponding to remaining Cr_2O_3, since the mesoporous material is purely organic.*

3. Characterization methods

Focused Ion Beam-Scanning Electron Microscopy (FIB-SEM). FIB-SEM sample preparation was performed in a DualBeam FEI Quanta 3D FEG microscope which combines a high-resolution Field Emission Gun SEM column with a high current Ga liquid metal ion gun FIB column. The procedure followed is illustrated in Figure S5. A protective layer of Pt was deposited on the area of interest using the gas injection system. Subsequently, the FIB was used to carve a thin slice of *ca* 2 µm-wide on the surface of the material (**2**).

An Omniprobe micro manipulator was used to hold the slice by platinum welding (**3**) and the slice was completely trimmed from the sample (**4-5**). Then, the slice was welded on a copper grid by using Pt (**6-7**). Finally, one section of the slice was finely milled in order to reduce the thickness to 200 nm, which allows the further analysis by TEM (**8-12**).

Transmission Electron Microscopy (TEM). Transmission electron microscopy (TEM) experiments were performed in a JEOL JEM-2000FX S/TEM microscope with LaB6 emitter at 200kV with a 120 µm condenser lens aperture and 80 µm objective lens aperture inserted.

Aberration corrected STEM. STEM was performed in a FEI TITAN X-FEG (60−300) transmission electron microscope equipped with spherical aberration CEOS corrector for the electron probe.

N_2 sorption isotherms. The samples were analyzed in a Micromeritics ASAP (Accelerated Surface Area and Porosimetry) 2020 System. Samples were weighted into tubes with seal frits and degassed under vacuum (<500 µm Hg) with heating. They were initially heated at 150 °C and held for 4 hours, and finally cooled to room temperature and backfilled with N_2. The samples were re-weighted before analysis. The analysis adsorptive was N_2 at 77K. A multi-point BET surface area was determined from 6 measurements at relative pressures (P/Po) ranging from 0.050 to 0.300. Single point adsorption total pore volume was measured near saturation pressure (Po ≈ 770 mmHg). Adsorption average pore width was also calculated.

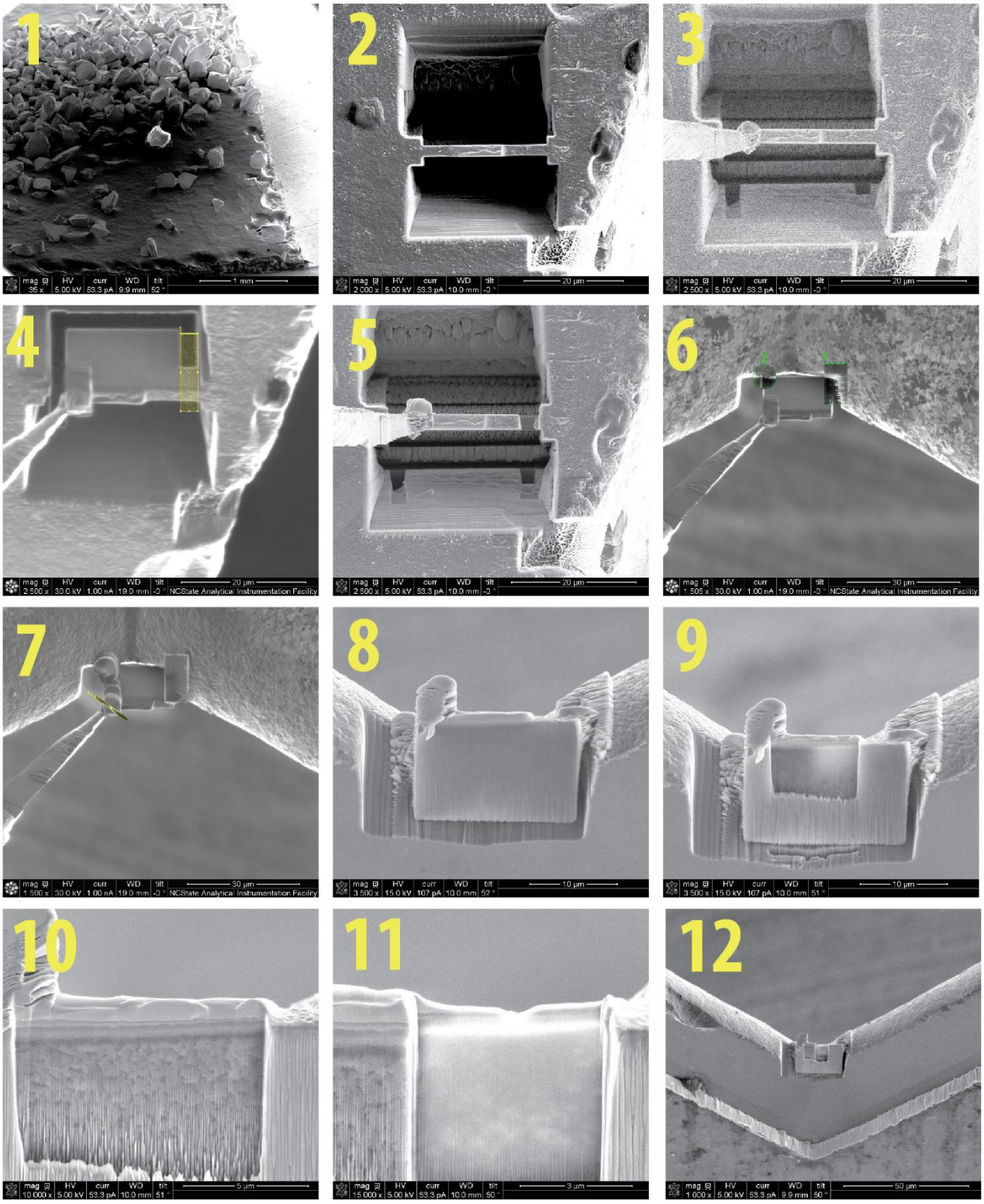

Figure S5. FIB-SEM preparation of the sample for TEM analysis.

X-ray fluorescence. XRF analysis were performed in a ARL Thermo Scientific (Ecublens, Switzerland) Perform'X Wavelength-Dispersive X-ray Fluorescence (WDXRF) equipped with an X-ray tube 5GN-type Rh target with ultra-thin 30 µm Be window to maximize light element response**.** 4000 W power supply for 60 kV max or 120 mA max with two detectors (flow proportional and scintillation) and seven analyzer crystals to achieve a broad elemental range**.** Sample data were processed using UniQuant, a standard-less software package that uses advanced fundamental parameters algorithms to determine elemental concentrations. Analysis is for seventy-nine elements and those elements above ten times the instrument calculated uncertainty are reported.

X-ray diffraction. XRD was used to study the crystalline structure of the MOF/MPM hybrid materials. XRD patterns were recorded using a Panalytical Empyrean X-ray diffractometer with Cu Kα radiation (λ=1.54778 Å). The samples were prepared by filling the holder with the dry powder. Phase formation and phase transition behaviors of the UiO-66(NH_2) powder were investigated using an XRK900 high temperature oven chamber. Sample was first heated in the chamber from 25 ^oC to 120 ^oC with a heating rate of 3 ^oC/min and held at 120 ^oC for 12 hours. After that, sample was cooled to room temperature with a cooling rate of 10 ^oC/min. Diffraction patterns were measured throughout the whole heat treatment using Cu Kα x-ray radiation with a wavelength of 1.5418 Å and a 2θ range of 4.5^o – 12^o. Each pattern was measured for 4 minutes using a step size and count time of 2θ = 0.0263^o and 147 sec/step, respectively.

FTIR: ATR and DRIFTS cell

ATR absorption spectroscopy measurements were performed in the range of 4000–400 cm^{-1} with a Perkin Elmer Spectrum 100 FTIR spectrometer. The 'in situ' DRIFTS experiments were carried out in a Praying Mantis cell by injecting a nitrogen flow saturated with water for assisting the solid-state synthesis at 120 °C.

Particle attrition measurements using a jet cup

Jet cup attrition testing is a common method for evaluating particle attrition in fixed fluidized beds and circulating fluidized beds. Davidson attrition index for (Cr)MIL-101(SO_3H)/Silica(A), (Cr)MIL-101(SO_3H) and Silica(A) has been determined by following the standard procedure[17].

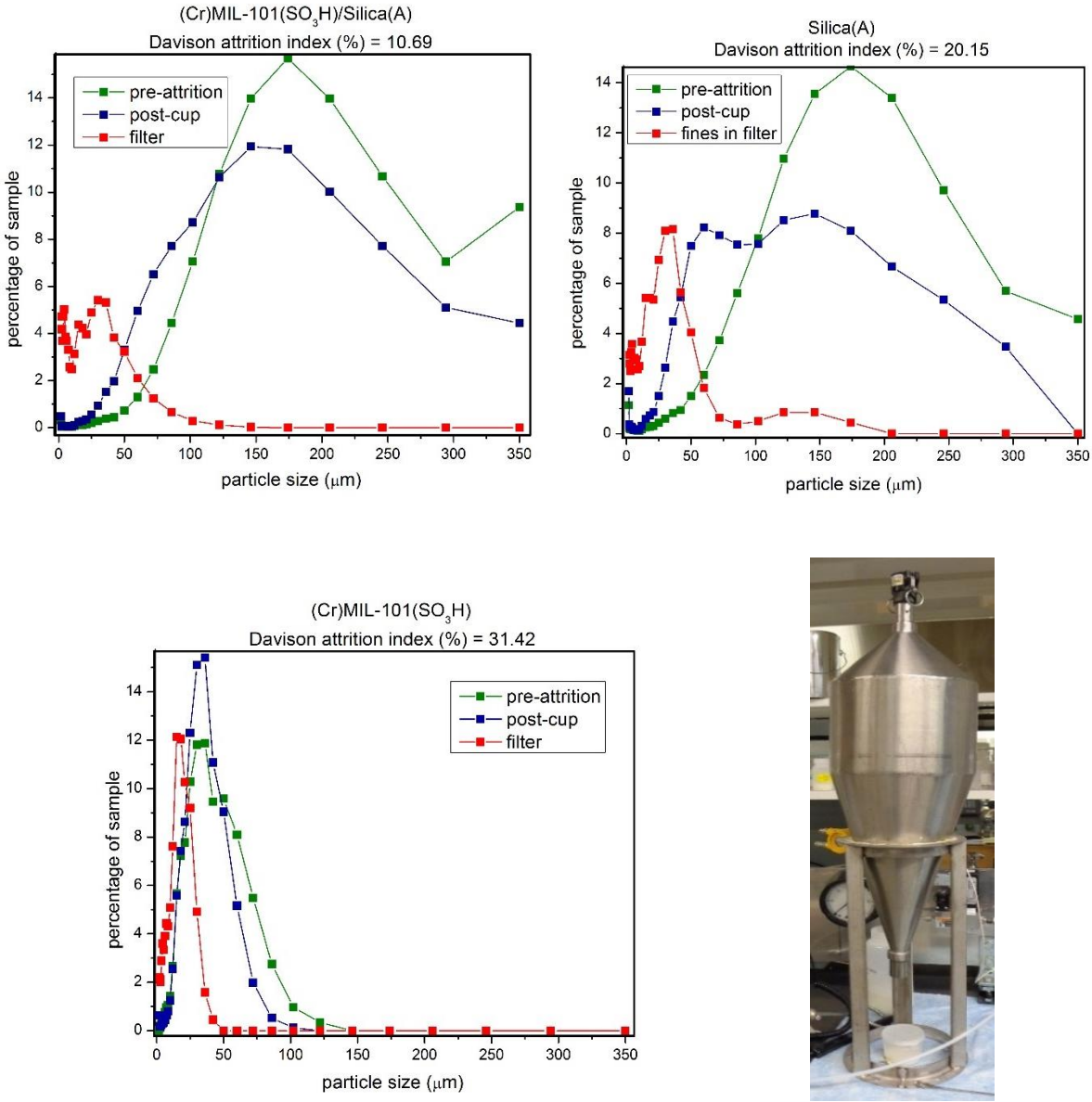

Figure S6. Davison Jet cup attrition test for (Cr)MIL-101(SO_3H)/Silica(A), (Cr)MIL-101(SO_3H) and Silica(A).

4. ‘In situ’ monitoring solid state MOF synthesis by DRIFTS and powder X-ray thermodiffraction

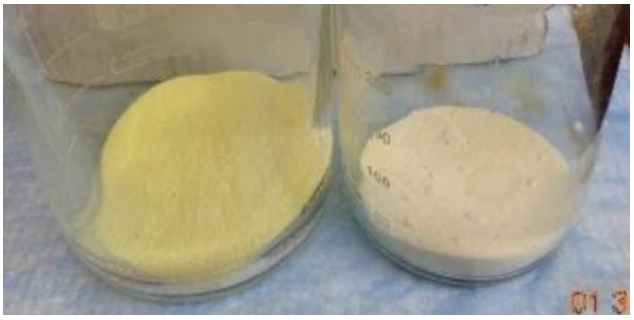

Figure S7. Example of color change of dry solid containing UiO-66(NH_2) precursors on silica A (intense yellow, left) and after solid-state synthesis for 2 hours at 120 °C in the oven (pale yellow, right).

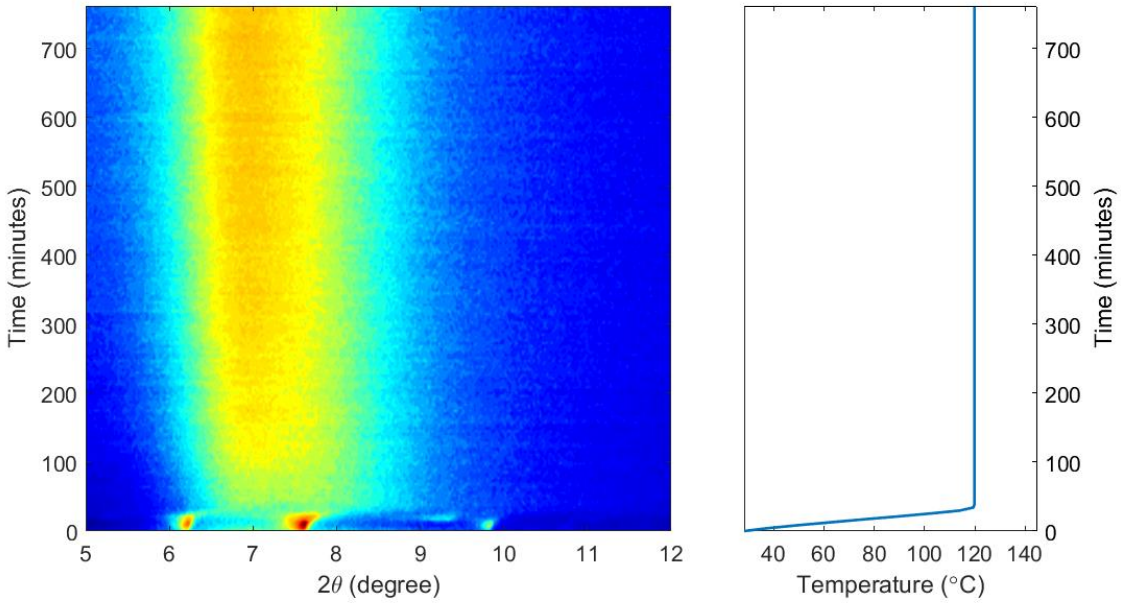

Figure S8a. Thermo-XRD diffraction spectra and temperature profile.

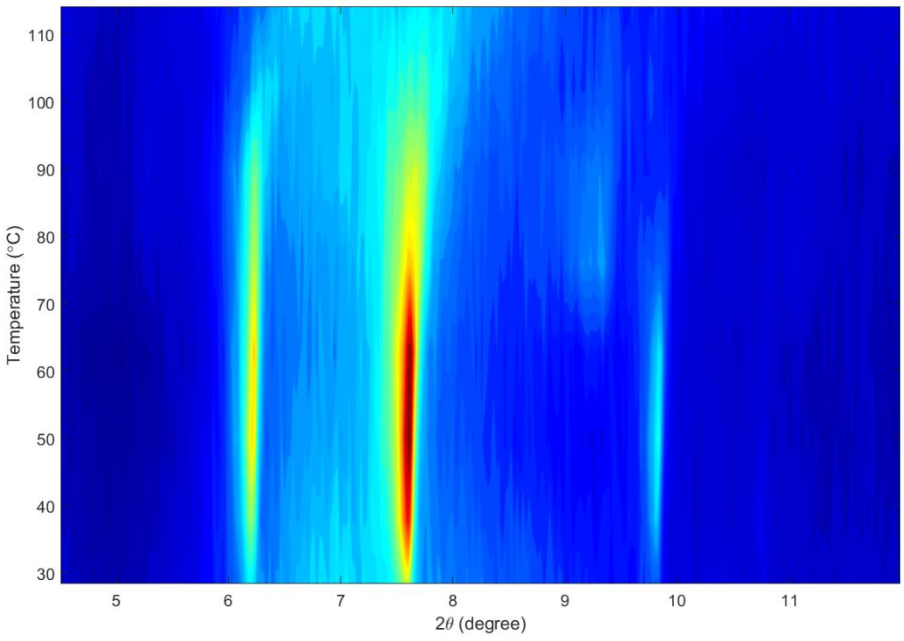

Figure S8b. Expanded area of Figure S9a during heating ramp during early 40 minutes showing an 'ephemeral' crystalline phase which disappears at higher temperatures.

5. Fourier Filtered Transformation (FFT) of a STEM-HAADF image of (Cr)MIL-101(SO_3H)/SBA-15

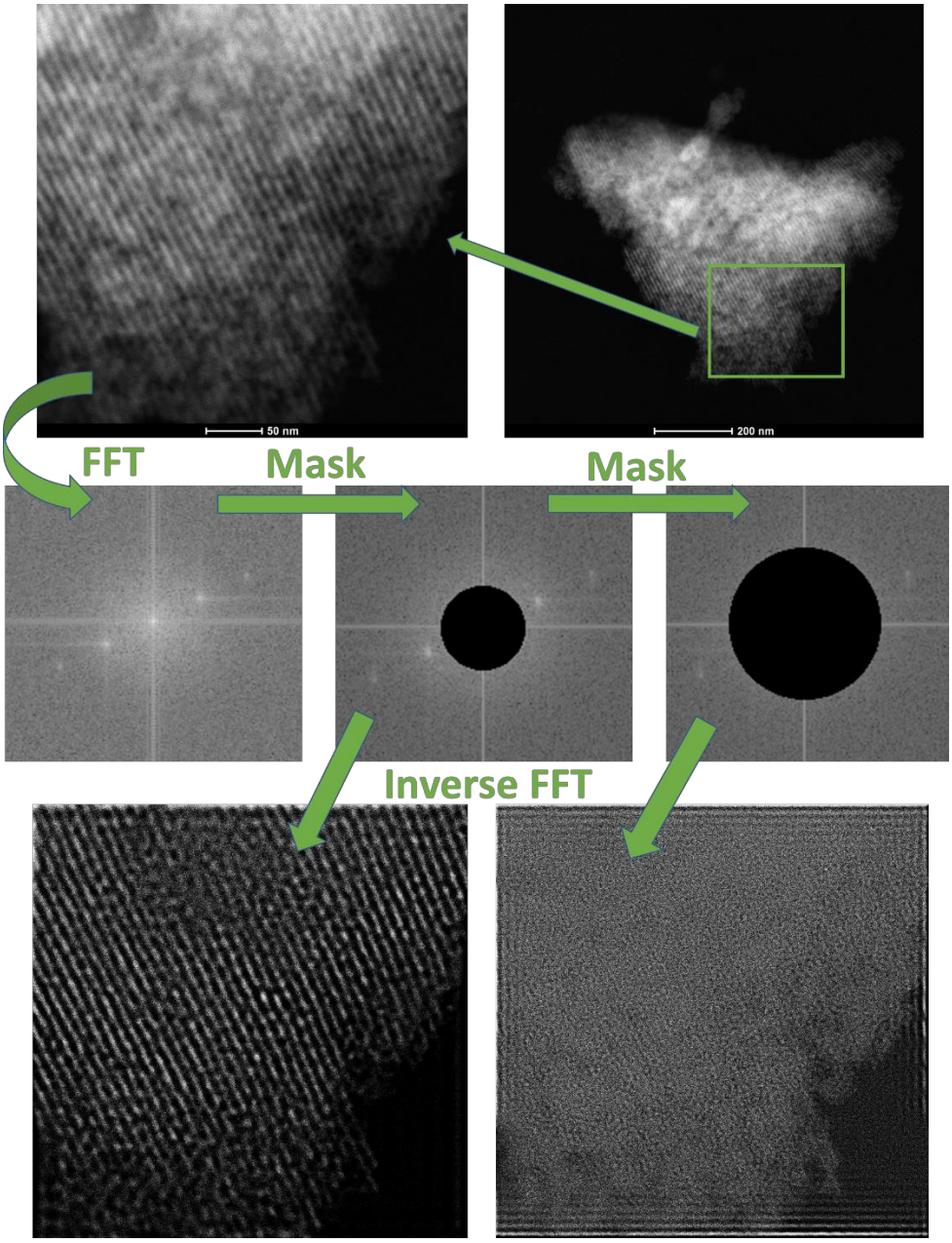

Figure S9. Fourier Filtered Transformation (FFT) of a STEM-HAADF image of MOF nanocrystals confined within SBA-15 [(Cr)MIL-101(SO_3H)/SBA-15].

Supplementary references

(1) Deria, P.; Bury, W.; Hupp, J. T.; Farha, O. K.: Versatile functionalization of the NU-1000 platform by solvent-assisted ligand incorporation. *Chem. Commun.* **2014**, *50*, 1965-1968.

(2) Zhao, D. Y.; Feng, J. L.; Huo, Q. S.; Melosh, N.; Fredrickson, G. H.; Chmelka, B. F.; Stucky, G. D.: Triblock copolymer syntheses of mesoporous silica with periodic 50 to 300 angstrom pores. *Science* **1998**, *279*, 548-552.

(3) Ferey, G.; Mellot-Draznieks, C.; Serre, C.; Millange, F.; Dutour, J.; Surble, S.; Margiolaki, I.: A chromium terephthalate-based solid with unusually large pore volumes and surface area. *Science* **2005**, *309*, 2040-2042.

(4) Serre, C.; Millange, F.; Thouvenot, C.; Noguès, M.; Marsolier, G.; Louër, D.; Férey, G.: Very Large Breathing Effect in the First Nanoporous Chromium(III)-Based Solids: MIL-53 or CrIII(OH)·{O2C−C6H4−CO2}·{HO2C−C6H4−CO2H}x·H2Oy. *J. Am. Chem. Soc.* **2002**, *124*, 13519-13526.

(5) Long, P. P.; Wu, H. W.; Zhao, Q.; Wang, Y. X.; Dong, J. X.; Li, J. P.: Solvent effect on the synthesis of MIL-96(Cr) and MIL-100(Cr). *Microporous Mesoporous Mater.* **2011**, *142*, 489-493.

(6) Juan-Alcaniz, J.; Gielisse, R.; Lago, A. B.; Ramos-Fernandez, E. V.; Serra-Crespo, P.; Devic, T.; Guillou, N.; Serre, C.; Kapteijn, F.; Gascon, J.: Towards acid MOFs - catalytic performance of sulfonic acid functionalized architectures. *Catal. Sci. Technol.* **2013**, *3*, 2311-2318.

(7) Volkringer, C.; Popov, D.; Loiseau, T.; Férey, G.; Burghammer, M.; Riekel, C.; Haouas, M.; Taulelle, F.: Synthesis, Single-Crystal X-ray Microdiffraction, and NMR Characterizations of the Giant Pore Metal-Organic Framework Aluminum Trimesate MIL-100. *Chem. Mater.* **2009**, *21*, 5695-5697.

(8) Couck, S.; Denayer, J. F. M.; Baron, G. V.; Remy, T.; Gascon, J.; Kapteijn, F.: An Amine-Functionalized MIL-53 Metal-Organic Framework with Large Separation Power for CO2 and CH4. *J. Am. Chem. Soc.* **2009**, *131*, 6326-+.

(9) Dietzel, P. D. C.; Morita, Y.; Blom, R.; Fjellvåg, H.: An In Situ High-Temperature Single-Crystal Investigation of a Dehydrated Metal–Organic Framework Compound and Field-Induced Magnetization of One-Dimensional Metal–Oxygen Chains. *Angew. Chem., Int. Ed.* **2005**, *44*, 6354-6358.

(10) Dietzel, P. D. C.; Panella, B.; Hirscher, M.; Blom, R.; Fjellvag, H.: Hydrogen adsorption in a nickel based coordination polymer with open metal sites in the cylindrical cavities of the desolvated framework. *Chem. Commun.* **2006**, 959-961.

(11) Kandiah, M.; Nilsen, M. H.; Usseglio, S.; Jakobsen, S.; Olsbye, U.; Tilset, M.; Larabi, C.; Quadrelli, E. A.; Bonino, F.; Lillerud, K. P.: Synthesis and Stability of Tagged UiO-66 Zr-MOFs. *Chem. Mater.* **2010**, *22*, 6632-6640.

(12) Fei, H.; Cohen, S. M.: A robust, catalytic metal-organic framework with open 2,2[prime or minute]-bipyridine sites. *Chem. Commun.* **2014**, *50*, 4810-4812.

(13) Kozachuk, O.; Luz, I.; Llabrés i Xamena, F. X.; Noei, H.; Kauer, M.; Albada, H. B.; Bloch, E. D.; Marler, B.; Wang, Y.; Muhler, M.; Fischer, R. A.: Multifunctional, Defect-Engineered Metal–Organic Frameworks with Ruthenium Centers: Sorption and Catalytic Properties. *Angew. Chem., Int. Ed.* **2014**, *53*, 7058-7062.

(14) Cravillon, J.; Münzer, S.; Lohmeier, S.-J.; Feldhoff, A.; Huber, K.; Wiebcke, M.: Rapid Room-Temperature Synthesis and Characterization of Nanocrystals of a Prototypical Zeolitic Imidazolate Framework. *Chem. Mater.* **2009**, *21*, 1410-1412.

(15) Dawei Feng; Zhi-Yuan Gu; Jian-Rong Li; Hai-Long Jiang; ZhangwenWei; Zhou, H.-C.: Zirconium-Metalloporphyrin PCN-222: Mesoporous Metal-Organic Frameworks with Ultrahigh Stability as Biomimetic Catalysts. *Angew. Chem., Int. Ed.* **2012**, *51*, 10307 -10310.

(16) McDonald, T. M.; Mason, J. A.; Kong, X. Q.; Bloch, E. D.; Gygi, D.; Dani, A.; Crocella, V.; Giordanino, F.; Odoh, S. O.; Drisdell, W. S.; Vlaisavljevich, B.; Dzubak, A. L.; Poloni, R.; Schnell, S. K.; Planas, N.; Lee, K.; Pascal, T.; Wan, L. W. F.; Prendergast, D.; Neaton, J. B.; Smit, B.; Kortright, J. B.; Gagliardi, L.;

Bordiga, S.; Reimer, J. A.; Long, J. R.: Cooperative insertion of CO2 in diamine-appended metal-organic frameworks. *Nature* **2015**, *519*, 303-+.

(17) Cocco, R.; Arrington, Y.; Hays, R.; Findlay, J.; Karri, S. B. R.; Knowlton, T. M.: Jet cup attrition testing. *Powder Technol.* **2010**, *200*, 224-233.